

On the Need for a Language Describing Distribution Shifts: Illustrations on Tabular Datasets

Jiashuo Liu^{1,*}, Tianyu Wang^{2,*}, Peng Cui¹, Hongseok Namkoong²

Tsinghua University¹

Columbia University²

liujiashuo77@gmail.com, tw2837@columbia.edu
cuip@tsinghua.edu.cn, namkoong@gsb.columbia.edu

Abstract

Different distribution shifts require different algorithmic and operational interventions. Methodological research must be grounded by the specific shifts they address. Although nascent benchmarks provide a promising empirical foundation, they *implicitly* focus on covariate shifts, and the validity of empirical findings depends on the type of shift, e.g., previous observations on algorithmic performance can fail to be valid when the $Y|X$ distribution changes. We conduct a thorough investigation of natural shifts in 5 tabular datasets over 86,000 model configurations, and find that $Y|X$ -shifts are most prevalent. To encourage researchers to develop a refined language for distribution shifts, we build WHYSHIFT, an empirical testbed of curated real-world shifts where we characterize the type of shift we benchmark performance over. Since $Y|X$ -shifts are prevalent in tabular settings, we identify covariate regions that suffer the biggest $Y|X$ -shifts and discuss implications for algorithmic and data-based interventions. Our testbed highlights the importance of future research that builds an understanding of how distributions differ.¹

1 Introduction

The performance of predictive models has been observed to degrade under distribution shifts in a wide range of applications, such as healthcare [8, 68, 56, 67], economics [28, 18], education [5], vision [55, 47, 64, 70], and language [46, 6]. Distribution shifts vary in type, typically defined as either a change in the marginal distribution of the covariates (X -shifts), or changes in the conditional relationship between the outcome and covariate ($Y|X$ -shifts). Real-world scenarios comprise of both types of shifts. In computer vision [46, 37, 60, 30, 72], $Y|X$ -shifts are less likely as Y is constructed from human labels given an input X . Due to the prevalence of X -shifts, the implicit goal of many researchers is to develop a single robust model that can generalize effectively across multiple domains, akin to humans.

For tabular data, $Y|X$ -shifts may arise because of missing variables and hidden confounders. For example, the prevalence of diseases among patients may be affected by covariates that are not recorded in medical datasets but vary among individuals, such as lifestyle factors (e.g., diet, exercise, smoking status) and socioeconomic status [31, 74, 67]. Under $Y|X$ -shifts, there may be a fundamental trade-off between learning algorithms: to perform well on a target distribution, a model may have to *necessarily* perform worse on others. Algorithmically, typical methods for addressing $Y|X$ -shifts include distributionally robust optimization (DRO) [11, 63, 21, 59, 20] and causal learning methods [54, 7, 62, 36]. Operationally, the modeler can identify and collect an unobserved confounder

¹More information on the data, codes and python packages about WHYSHIFT are available at <https://github.com/namkoong-lab/whyshift>.

*Equal contribution

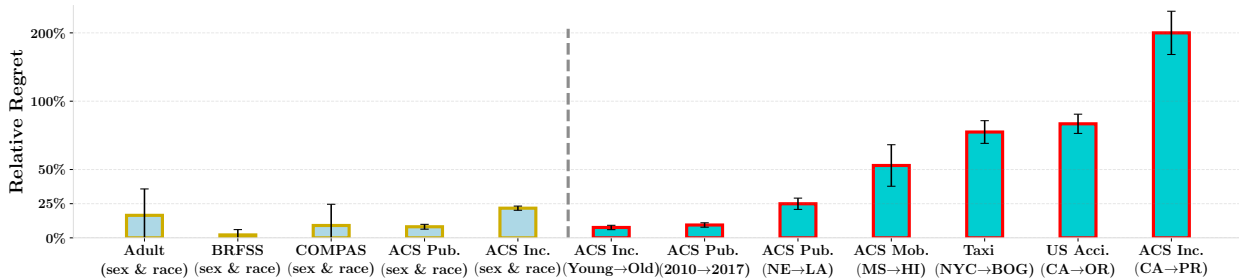


Figure 1. *Relative regret* (1.1) in typical benchmarks [19, 23] (*left 5 bars*) and seven settings designed in our benchmark (*right 7 bars*). We use XGBoost \mathcal{F} here for illustration.

C such that $Y|X, C$ remains invariant across domains, or resort to overhauling the entire model development pipeline to collect more samples from the target.

Although nascent benchmarks provide a promising foundation [55, 37, 18, 60], the distribution shift types in these datasets are poorly understood, underscoring the ambiguity in the external validity of the empirical findings based on them. For example, we find that previous (unqualified) empirical findings only hold over mild X -shifts, but fail to hold over $Y|X$ -shifts (Figure 2 to come). As the validity of empirical findings implicitly depends on the type of shift, it is essential to understand the patterns of real-world distribution shifts. Any methodological development must be grounded by the specific shifts it does and does not address.

In this work, we focus on tabular datasets to illustrate how a deeper understanding of the underlying shift is necessary for empirical rigor. As a motivating example, we consider tabular datasets that have been previously used to benchmark model performance over demographic subgroups: `Adult`, `BRFSS`, `COMPAS`, `ACS Public Coverage`, and `ACS Income` [3, 73, 23]. To understand the type of distribution shift introduced in these datasets, we take the largest demographic subgroup and the smallest subgroup (e.g., for `Adult`, white men as P and non-white women as Q), and study the optimality gap of the model f_P learned on P as measured on the target data Q . Formally, define the *relative regret* over the target distribution Q :

$$\frac{\mathbb{E}_Q[\ell(Y, f_P(X))]}{\min_{f \in \mathcal{F}} \mathbb{E}_Q[\ell(Y, f(X))]} - 1 \quad \text{where } f_P \in \operatorname{argmin}_{f \in \mathcal{F}} \mathbb{E}_P[\ell(Y, f(X))], \quad (1.1)$$

where we use 0-1 loss for $\ell(\cdot, \cdot)$ in Figure 1. For the widely-used benchmarks (left 5 bars), we observe that the relative regret is small, suggesting that the $Y|X$ distribution is *largely transferable* across those demographic groups and that X -shifts are mild.

Towards building an understanding of how empirical findings depend on the type of distribution shift, we present a testbed representing a diverse range of shifts. Our comprehensive benchmark is based on 5 real-world tabular datasets constructed from the US Census (as proposed by Ding *et al.* [18]) and traffic measurements [48, 49, 1, 2]. We carefully select 7 specific source-target pairs and characterize the extent of $Y|X$ -shifts in each setting. As we observe in Figure 1, our benchmarks cover a wide range of $Y|X$ -shifts and provide the following initial observations.

$Y|X$ -shifts are prevalent in tabular settings Through our benchmark, we highlight that $Y|X$ -shifts constitute a substantial proportion of real-world distribution shifts. Out of 169 source-target pairs with significant performance degradation (> 8 percentage points of accuracy drop), we find 80% of them are primarily attributed to $Y|X$ -shifts. By explicitly modeling $Y|X$ -shifts prevalent in applications, as shown in Figure 1, our benchmark enables a nuanced understanding of how empirical findings depend on the type of shift. In particular, we observe that $Y|X$ -shifts introduce considerable performance variation on the target distribution, leading to different relationships between in-

and out-of-distribution performances across settings and datasets. This is in stark contrast to the recently observed accuracy-on-the-line phenomenon [47], where the in- and out-of-distribution performance have been posited to exhibit a strong linear relationship. In Figure 2, we showcase how the accuracy-on-the-line trend fails to hold when $Y|X$ -shifts are strong.

We need tools that build a deeper understanding of distribution shifts There is a salient need for methodological research that builds a deep understanding of distributional differences. This is particularly important for $Y|X$ -shifts since in the worst case, the source data may not be informative for modeling the $Y|X$ relationship in the target, necessitating a full overhaul of the data collection and validation procedure. To inform algorithmic or operational interventions, we must understand *why* the distribution changed. Our empirical study in Section 3 underscores how identifying the causes behind $Y|X$ -shifts can help shape the solution space beyond the typical algorithmic interventions. We introduce a simple method that identifies covariate regions that have worse performance due to $Y|X$ -shifts. In our benchmark, we illustrate how our methodology suggests effective operational interventions: 1) collecting some target data over a particular covariate region, and 2) collecting specific features C such that the $Y|X, C$ distribution is more stable across source and target.

A comprehensive benchmark with specified shift patterns We construct WHYSHIFT, a benchmark for evaluating complex distribution shifts, encompassing six datasets and curated source-target transfer pairs. We call our benchmark WHYSHIFT since addressing $Y|X$ -shifts requires an understanding of *why* the distribution changed. We evaluate 22 methods on 7 specified distribution shifts with over 86,000 model configurations, comparing a broad range of algorithms including tree ensembles, DRO, imbalance, and fairness methods. We highlight our key findings.

- In tabular settings, model performance rankings change over different shift patterns.
- Tree ensemble methods are competitive, but still suffer from significant performance degradation.
- DRO methods are sensitive to configurations and exhibit significant performance variations.
- Imbalance and fairness methods show similar performance with the base learner (XGBoost).
- A small validation data from the target distribution goes a long way, and more generally, non-algorithmic interventions warrant greater consideration.

2 Distribution Shifts in Tabular Settings

To illustrate how complex distribution shift patterns arise in tabular data, we compare 22 algorithms including tree ensemble methods, robust learning, imbalance, and fairness methods. On 5 real-world tabular datasets (ACS Income, ACS Public Coverage (ACS Pub. Cov), ACS Mobility [18], US Accident [48, 49] and Taxi [1, 2]), we consider the natural spatial shifts between states/cities (e.g., California to Puerto Rico). For the ACS Pub.Cov dataset, we also consider temporal shifts, e.g., from 2010 to 2017. Since virtually all natural distribution shifts we consider are largely induced by $Y|X$ -shifts, we construct a synthetic subgroup shift from younger people to older people in order to simulate X -shifts. Deferring a detailed summary to Section 4.1, we focus on introducing representative phenomena in this section.

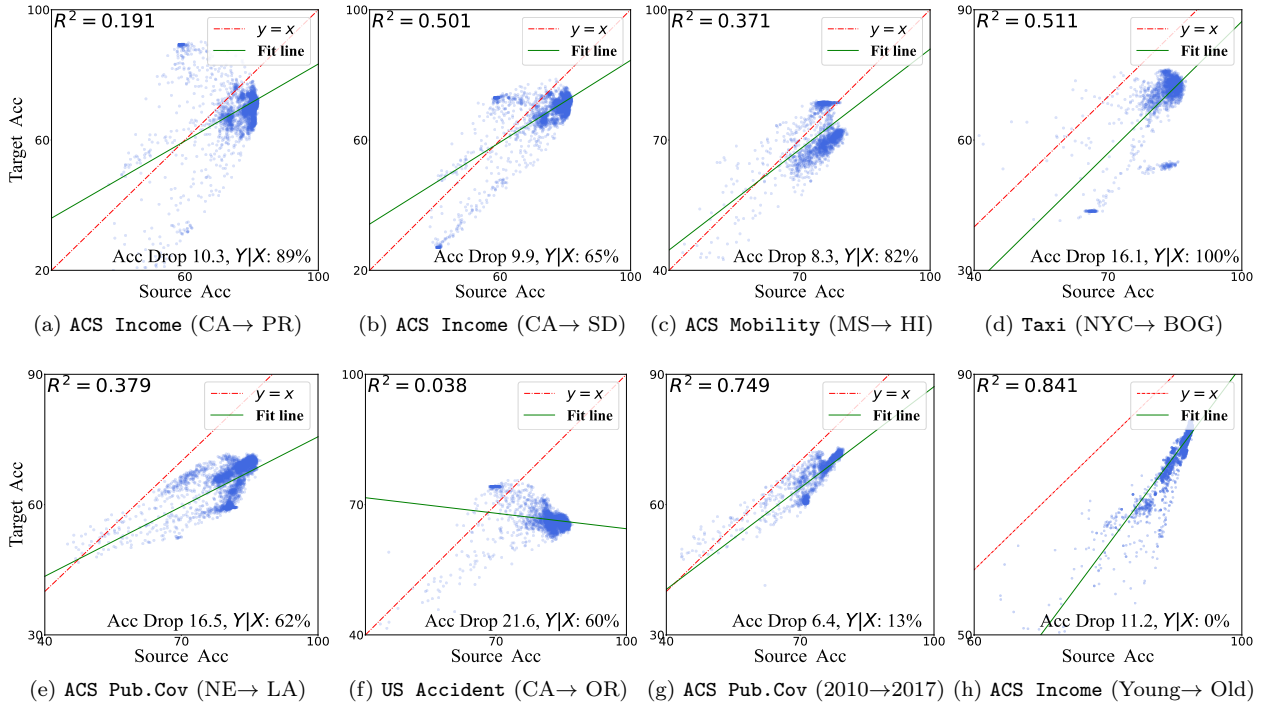


Figure 2. Target vs. source accuracies for 22 algorithms and datasets in our benchmark. A linear fit (green line) and its corresponding R^2 value is reported on the top left of each figure. Each blue point represents one hyperparameter configuration. **(a)-(b)**: two examples of ACS Income dataset with California (CA) as the source state, and Puerto Rico (PR) and South Dakota (SD) as targets. **(c)-(g)**: five examples of ACS Mobility, Taxi, ACS Pub.Cov, US Accident datasets. **(h)**: simulated covariate shifts on on sub-sampled ACS Income dataset.

In Figure 2, we present the source (in-distribution) and target (out-of-distribution) performances of 22 algorithms, each with 200 hyperparameter configurations. To understand shift patterns, we utilize the recently proposed Distribution Shift DEcomposition (DISDE) framework [13] which decomposes the performance degradation into components attributed to $Y|X$ - and X -shifts. Using the best XGBoost configuration as the baseline model for each source-target pair, we present the total performance degradation and the proportion attributed to $Y|X$ -shift.

Distribution shifts are predominantly $Y|X$ -shifts We find performance degradation under natural shifts is overwhelmingly attributed to $Y|X$ -shifts, as illustrated in the curated list in Figure 2. More generally, out of the 169 source-target pairs whose performance degradation is larger than 8 percentage points, 87.2% of them have over 50% of the performance degradation attributed to $Y|X$ -shifts (70.2% of them have over 60% of the gap attributed to $Y|X$ -shifts). We conjecture that $Y|X$ -shifts are prevalent in tabular data due to missing features. For example, in the context of income prediction, individual outcomes may change due to unobserved economic and political factors whose distribution changes over geographical locations [18]. In contrast, in vision and language tasks, the input (e.g., pixels and words) often encapsulate most of the necessary information for predicting the outcome, making strong $Y|X$ -shifts less likely unless the labeling noise is severe. Consequently, compared to domain generalization tasks in vision and language, tabular data exhibits more pronounced real $Y|X$ -shifts. Our findings highlight the importance of understanding the *cause*

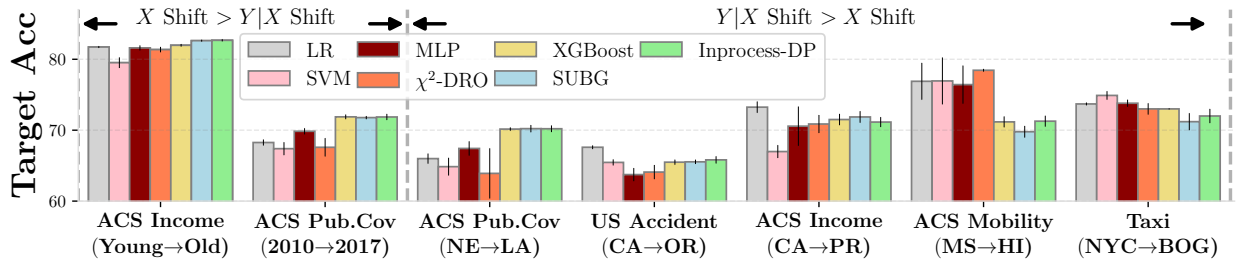


Figure 3: Performances of typical algorithms of 7 settings in our benchmark.

of the distribution shift.

Accuracy-on-the-line fails to hold over $Y|X$ -shifts We find significant variation in the relationship between source and target performance throughout all natural distribution shifts presented in Figure 2a-g. The correlation between source and target performance is relatively weak, and we tend to see poor linear fits (low R^2) when the bulk of the performance degradation is attributed to $Y|X$ -shifts. In Figure 2a-b where we study models trained on California data, we see a significant decrease in the correlation as $Y|X$ -shifts become stronger (SD to PR). Similarly, we see in Figures 2 (c)-(f) that the relationship between the two performances exhibits significant fluctuations across different source-target pairs. In Figure 3, we observe performance rankings of algorithms substantially vary across different $Y|X$ -shifts. Our finding highlights the inherent complexity associated with real distribution shifts in tabular datasets, which stands in sharp contrast to the “accuracy-on-the-line” phenomena [47]. The varied shift patterns in tabular data highlight how empirical observations must be qualified over the range of shifts they remain valid over. This is particularly important for $Y|X$ -shifts which introduce larger variations in the relationship between source and target performance.

Source and target performances are correlated when X -shifts dominate Across all natural shifts we study, we find X -shifts are only prominent in temporal shifts (ACS Time dataset; Figure 2g) To better investigate the role of X -shifts, we subsample the data to artificially induce strong covariate shifts over an individual’s age. Specifically, we focus on individuals from California and form two groups according to whether their age is ≥ 25 . The source data oversamples low age groups where 80% is drawn from the age ≤ 25 group; proportions are reversed in the target data.

On this synthetic shift we construct, the DISDE [13] method attributes the bulk of the performance degradation to X -shifts in Figure 2h. Our finding confirms the intuition that unobserved economic factors remain relatively consistent for individuals from the same state (CA). In this synthetic example with X -shifts, we observe a relatively strong correlation between source and target performance. Moreover, the large performance degradation on these datasets suggests that existing robust learning methods are still severely affected by covariate shifts, indicating the need for future research that addresses covariate shifts in tabular data.

3 Case Study: Understanding Distribution Shifts Facilitates Interventions

Typical algorithmic approaches to distribution shift optimize performance over a postulated set of distribution shifts. Causal learning assumes the underlying causal structure can be learned to withstand distribution shift [54, 62, 61, 57], while DRO methods explicitly optimize worst-case

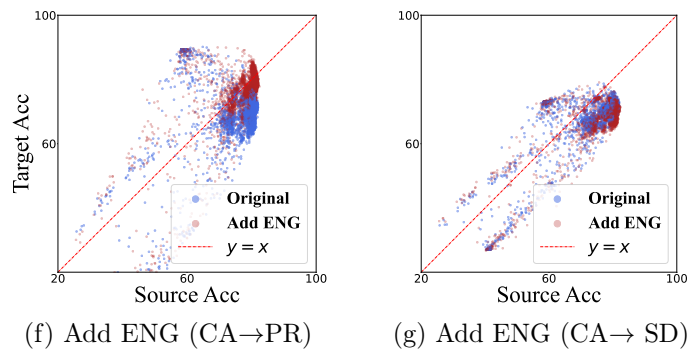
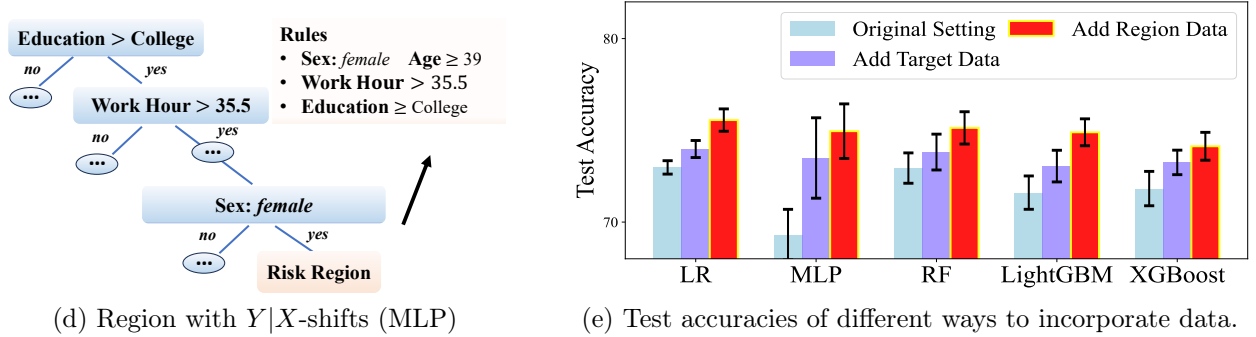
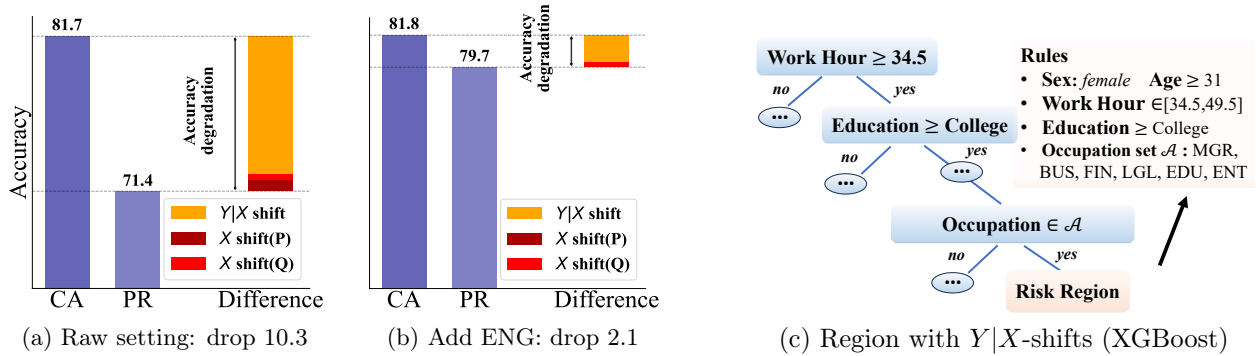


Figure 4. Case study illustrations. (a)-(b) Decomposition of performance degradation for the XGBoost classifier from CA to PR. Figure (a) is for the original setting and (b) corresponds to the results post-integration of the "ENG" feature. (c)-(d) Demonstration of Algorithm 1: an interpretable version of the region with strong $Y|X$ -shifts for the XGBoost and MLP models, respectively. (e) Test accuracies of five typical base methods trained on the source, post addition of 250 randomly selected *target observations*, and 250 observations from the identified *risk region*. (f)-(g) Performances of all algorithms prior to and following the addition of the "ENG" feature. Figure (f) corresponds to the CA to PR, and Figure (g) is CA to SD.

Algorithm 1: Identify Regions with Strong $Y|X$ -Shifts.

Input: Source samples $(X_i, Y_i) \stackrel{\text{i.i.d.}}{\sim} P$, with size n_P and target samples $(X_j, Y_j) \stackrel{\text{i.i.d.}}{\sim} Q$ with size n_Q . Model discrepancy threshold b .

- 1 Estimate $\hat{\pi}(x) = \mathbb{P}(\tilde{X} \sim Q_x | \tilde{X} = x)$ by training a classifier on source and target samples.
- 2 Calculate density ratios \hat{s}_X/p_X and \hat{s}_X/q_X according to Equation (3.3).
- 3 Fit prediction models f_P and f_Q according to Equation (3.4) and (3.5).
- 4 Using weighted samples from S_X , fit a shallow decision tree $h(x)$ to predict $|f_P(x) - f_Q(x)|$.

Output: Region $R = \{x \in \mathcal{X} : h(x) \geq b\}$.

performance over a set of distributions [11, 39, 21, 20]. Despite progress in algorithm design, there are few efforts that examine the patterns of real-world distribution shifts. It remains unclear whether the data assumptions made by algorithms hold in practice, and this *mismatch* often leads to poor empirical performance [32, 68, 56, 14, 36].

Complementing the active literature on algorithmic development, we present an empirical study that underscores the practical significance of tools that provide a qualitative understanding of the shift at hand. In light of the prevalence of $Y|X$ -shifts in tabular data, we introduce a simple yet effective approach for identifying covariate regions that suffer strong $Y|X$ -shifts. We demonstrate our approach on the income prediction task (**ACS Income**), and show that it can guide operational interventions for addressing distribution shifts. Our case study is not meant to be a rigorous scientific analysis, but rather a (heuristic) vignette illustrating the need for future research on methodologies that can generate qualitative insights on distributional differences.

3.1 Identifying Regions with Strong $Y|X$ -shifts

Here we propose a simple yet effective method for identifying covariate regions with strong $Y|X$ -shifts. Despite its simplicity, we demonstrate in the following subsections that our method can inspire operational and modeling interventions. Consider a model $f : \mathcal{X} \rightarrow \mathcal{Y}$ that predicts outcome $Y \in \mathcal{Y}$ from covariates $X \in \mathcal{X}$ with the associated loss function $\ell(f(X), Y)$. Our goal is to identify a region $\mathcal{S} \subseteq \mathcal{X}$ where $P(Y|X)$ differs a lot from $Q(Y|X)$. Since $P(Y|X)$ and $Q(Y|X)$ are undefined outside of the support of $P(X)$ and $Q(X)$ respectively, the comparison can only be made on a subset of the common support. To operationalize this notion of common support, we construct a *shared distribution* S_X over X whose support is contained in that of P_X and Q_X (following [13]).

Let p_X, q_X be the densities of X under P, Q . We define the shared density s_X as

$$s_X(x) \propto p_X(x)q_X(x)/(p_X(x) + q_X(x)). \quad (3.1)$$

Since we do not have access to samples from the shared distribution S_X , we reweight samples from P_X and Q_X using the likelihood ratios $s_X(x)/p_X(x) \propto q_X(x)/(p_X(x) + q_X(x))$ and $s_X(x)/q_X(x) \propto p_X(x)/(p_X(x) + q_X(x))$. Noting that the ratio can be modeled as the probability that an input x is from P_X vs Q_X , we train a binary “domain” classifier to estimate the ratios. The “domain” classifier can be any black-box method, and we use XGBoost throughout. Empirically, given that the numbers

of samples from P_X and Q_X may differ (*i.e.*, $n_P \neq n_Q$), we have:

$$\hat{\alpha} = \frac{n_Q}{n_P + n_Q} \quad \text{and} \quad \hat{\pi}(x) = \mathbb{P}(\tilde{X} \text{ from } Q_X | \tilde{X} = x), \quad (3.2)$$

$$\frac{\hat{s}_X}{p_X}(x) \propto \frac{\hat{\pi}(x)}{(1 - \hat{\alpha})\hat{\pi}(x) + \hat{\alpha}(1 - \hat{\pi}(x))} \quad \text{and} \quad \frac{\hat{s}_X}{q_X}(x) \propto \frac{1 - \hat{\pi}(x)}{(1 - \hat{\alpha})\hat{\pi}(x) + \hat{\alpha}(1 - \hat{\pi}(x))}. \quad (3.3)$$

We estimate the best prediction model under P and Q over the shared distribution S_X (using XGBoost as the model class \mathcal{F})

$$f_P := \arg \min_{f \in \mathcal{F}} \mathbb{E}_{S_X} \left[\mathbb{E}_P[\ell(f(X), Y) | X] \right] = \mathbb{E}_P \left[\ell(f(X), Y) \frac{dS_X}{dP_X}(X) \right], \quad (3.4)$$

$$f_Q := \arg \min_{f \in \mathcal{F}} \mathbb{E}_{S_X} \left[\mathbb{E}_Q[\ell(f(X), Y) | X] \right] = \mathbb{E}_Q \left[\ell(f(X), Y) \frac{dS_X}{dQ_X}(X) \right]. \quad (3.5)$$

Then, for any threshold $b \in [0, 1]$, $\{x \in \mathcal{X} : |f_P(x) - f_Q(x)| \geq b\}$ suggests a region that may suffer model performance degradation due to $Y|X$ -shifts.

To allow simple interpretation, we use a shallow *decision tree* $h(x)$ to approximate $|f_P(x) - f_Q(x)|$ on the *shared distribution* S_X , and consider $\{x \in \mathcal{X} : h(x) \geq b\}$ given by the leaf node of the tree. The pseudo-code is shown in the Algorithm 1; we show that the node splitting criterion in a standard decision trees training procedure corresponds with our goal of finding regions with the largest discrepancy in Appendix B.2.

3.2 Model Interventions

Using Algorithm 1, we now demonstrate how a better understanding of distribution shifts can facilitate the design of interventions. We focus on the ACS Income dataset where the goal is to predict whether an individual’s income exceeds 50k (Y) based on their tabular census data (X). We train an income classifier on 20,000 samples from California (CA, source), and deploy the classifier in Puerto Rico and South Dakota (PR & SD, target), where we get 4,000 samples from PR and SD after deployment. Given the considerable disparities in the economy, job markets, and cost of living between CA and PR/SD, we observe substantial performance degradation due to distribution shifts.

In Figure 4a, we first decompose the performance degradation from CA to PR to understand the shift and find $Y|X$ -shifts are the predominant factor. We dive deeper into the significant $Y|X$ -shifts and identify from CA to PR for the XGBoost and MLP classifier. From the region shown in Figure 4c and Figure 4d, we find college-educated individuals in business and educational roles (such as management, business, and educational work) exhibit large $Y|X$ differences.

To illustrate how our analysis can inspire subsequent operational interventions to enhance performance on the target distribution, we study two operational interventions.

Collect specific data from the target To improve target performance, the most natural operational intervention is to collect additional data from the target distribution. While a rich body of work on domain adaptation [51, 16, 22, 66, 65] study how to effectively utilize data from the target distribution to improve performance, there is little work that discusses how to efficiently collect supervised data from the target distribution to maximize out-of-distribution generalization. To highlight the need for future research in this space, we use the interpretable region identified by Algorithm 1 as shown in Figure 4c to simulate a concerted data collection effort.

Table 1: Overview of datasets and 7 selected settings.

#ID	Dataset	Type	#Samples	#Features	Outcome	#Domains	Selected Settings	Shift Patterns
1	ACS Income	Natural	1,599,229	9	Income \geq 50k	51	California \rightarrow Puerto Rico	$Y X \gg X$
2	ACS Mobility	Natural	620,937	21	Residential Address	51	Mississippi \rightarrow Hawaii	$Y X \gg X$
3	Taxi	Natural	1,506,769	7	Duration time \geq 30 min	4	New York City \rightarrow Botogá	$Y X \gg X$
4	ACS Pub.Cov	Natural	1,127,446	18	Public Ins. Coverage	51	Nebraska \rightarrow Louisiana	$Y X > X$
5	US Accident	Natural	297,132	47	Severity of Accident	14	California \rightarrow Oregon	$Y X > X$
6	ACS Pub.Cov	Natural	859,632	18	Public Ins. Coverage	4	2010 (NY) \rightarrow 2017 (NY)	$Y X < X$
7	ACS Income	Synthetic	195,665	9	Income \geq 50k	2	Younger \rightarrow Older	$Y X \ll X$

Since indiscriminately collecting data from the target distribution can be resource-intensive, we concentrate sampling efforts on the subpopulation that may suffer from $Y|X$ -shifts and selectively gather data on them. For five base methods (logistic regression, MLP, random forest, lightGBM, and XGBoost), we randomly sample 250 points from the whole target distribution and the identified region suffering prominent $Y|X$ -shifts, respectively. We report the test accuracies in Figure 4e, and observe that incorporating data from this region is more effective in enhancing OOD generalization. While preliminary, our results demonstrate the potential robustness benefits of efficiently allocating resources toward concerted data collection. Future methodological research in this direction may be fruitful; potential connections may exist with active learning algorithms [69, 43, 27].

Add more relevant features We now illustrate the potential benefits of generating qualitative insights on the distribution shift at hand. Our analysis in Figure 4c suggests educated individuals in financial, educational, and legal professions tend to experience large $Y|X$ -shifts from CA to PR. These roles typically need communication skills, and language barriers could potentially affect their incomes. In California (CA), English is the primary language, while in Puerto Rico (PR), despite both English and Spanish being recognized as official languages, Spanish is predominantly spoken. Consequently, for a model trained on CA data and tested on PR data, incorporating a new feature that denotes English language proficiency (hereafter denoted “ENG”) might prove beneficial in improving generalization performances. However, this feature is not included in the ACS Income dataset.

To address this, we went back to the Census Bureau’s American Community Survey database to include the ENG feature in the set of covariates. In Figure 4b, we observe that the inclusion of this feature substantially reduces the degradation due to $Y|X$ -shifts, verifying that the originally missing ENG feature may be one cause of $Y|X$ -shifts. Figure 4f contrasts the performances of 22 algorithms (each with 200 hyperparameter configurations) with original features with those that additionally use the ENG feature. The new feature significantly improves target performances across all algorithms; roughly speaking, we posit that we have identified a variable C such that $Y|X, C$ remains similar across CA and PR. However, when we extend this comparison to the source-target pair CA \rightarrow SD, we observe no significant improvement (Figure 4g). This highlights that the selection of new features should be undertaken judiciously depending on the target distributions of interest. A feature that proves effective in one target distribution might not yield similar results in another.

4 WHYSHIFT: Benchmarking Distribution Shifts on Tabular Data

In this section, we detail our benchmark and summarize the main observations. Our finding highlights the importance of future research that builds an understanding of *why* the distribution shifted.

4.1 Setup

Datasets We explore distribution shifts on 5 real-world tabular datasets from the economic and traffic sectors with *natural* spatiotemporal distribution shifts. For economic data, we use **ACS Income**, **ACS Mobility**, and **ACS Public Coverage** datasets from the US-wide ACS PUMS data [18], where the outcome is whether an individual’s income exceeds 50k, whether an individual changed the residential address one year ago, and whether an individual is covered by public health insurance, respectively. We primarily focus on spatial shifts across different states in the US. To complement spatial shifts, we derive an **ACS Time** task based on the **ACS Public Coverage** dataset, where there are temporal shifts between different years (2010 to 2021). For traffic data, we use **US Accident** [48, 49] and **Taxi** [1, 2], where the outcome is whether an accident is severe and whether the total ride duration time exceeds 30 minutes, respectively. We focus on spatial shifts between different states/cities. We summarize the datasets in Table 1 and defer a full description to the Appendix C.1.

Algorithms We evaluate **22** algorithms that span a wide range of learning strategies on tabular data, and compare their performances under different patterns of distribution shifts we construct. Concretely, these algorithms include: (1) *base learners*: Logistic Regression, SVM, fully-connected neural networks (MLP) with standard ERM optimization; (2) *tree ensemble models*: Random Forest, XGBoost, LightGBM; (3) *robust learning*: CVaR-DRO and χ^2 -DRO with fast implementation [39], CVaR-DRO and χ^2 -DRO of outlier-robust enhancement [76], Group DRO [58]; (4) *imbalanced learning*: JTT [42], SUBY, RWY, SUBG, RWG [33], DWR [38] and (5) *fairness-enhancing methods*: inprocessing method [4] with demographic parity, equal opportunity, error parity as constraints, postprocessing method [29] with exponential and threshold controls. For DRO methods (i.e. (3)), we use MLP as the backbone model. For other algorithms compatible with tree ensemble models (i.e. (4-5)), we use the XGBoost model due to its superior performance on tabular data [26]. For algorithms requiring group labels, we use ‘hour’ for **US Accident** and **Taxi**, and ‘sex’ for the others. Detailed descriptions for each algorithm can be found in Appendix C.5.

Benchmarks We conduct experiments with more than 86,000 model configurations on various source-target distribution shift pairs, and carefully select 7 representative pairs with *different distribution shift patterns*. In Table 1, we introduce **7 selected settings**, and characterize the shift patterns of source-target pairs, which contain different proportions of $Y|X$ -shifts and X -shifts corresponding with plots in Figure 2. The first six settings are natural shifts. In the last setting, we sub-sample the dataset according to age to introduce covariate shift, where we focus on individuals from California and form two groups according to whether their age is ≥ 25 . The source data over-samples the low age group where 80% is drawn from the age ≥ 25 group, and the proportions are reversed in the target data.

In Figure 5 and Figure 6, we plot the performance of algorithms using their best hyperparameter configuration on the validation dataset (*i.i.d.* with the source distribution). Additional results with various source distributions are in the Appendix. Our benchmark is designed to support empirical research, including new learning algorithms and diagnostics that provide qualitative insights on distribution shifts.

Hyper-parameter Tuning For each model, we conduct a grid search over a large set of hyper-parameters. (See Appendix C.3 for the complete search space for each method.) When one method includes another as a “base” learner (e.g., DRO with MLP, RWY with XGBoost), we explore the full tuning space for the base model (e.g., the cross-product of all MLP hyper-parameters with all DRO hyper-parameters). To control for computational effort, each method is run with 200 configurations for each source-target pair and we select the best configuration according to the *i.i.d.*

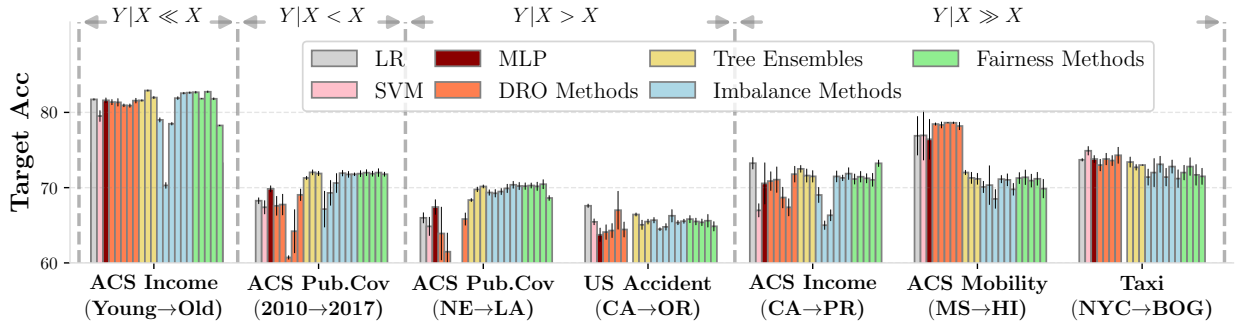


Figure 5: Overall performances of all algorithms on the target data in our selected 7 settings.

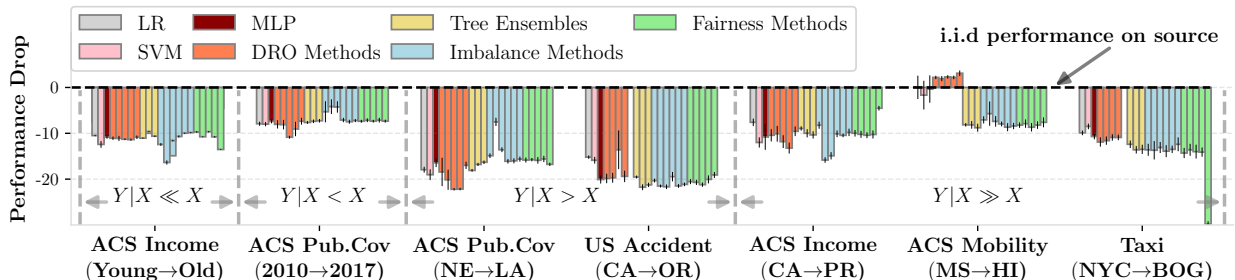


Figure 6. Performance drop between source and target data of all algorithms in our selected 7 settings.

validation performance. In Figure 7b, we further compare different choices of validation protocols.

Evaluation Metrics In our benchmark, we include different metrics for a thorough evaluation. Specifically, we use Average Accuracy, Worst-group Accuracy, and Macro-F1 score in our main results where we only have one target distribution. For the results with multiple target distributions (i.e. 3 in Taxi, 13 in US Accident and 50 in the others), we present *all* target accuracies and Macro-F1 scores, as well as the worst-distribution accuracy and Macro-F1 score among all target distributions in Appendix C.6, C.7, C.8, C.9.

4.2 Analysis

Different algorithms do not exhibit consistent rankings over different shift patterns. In Figure 5, we observe the rankings across different shifts are quite different, especially for ACS Income (CA→PR) and ACS Mobility (MS→HI) where $Y|X$ -shifts dominate. This observation reaffirms the phenomena in Figure 2 that as $Y|X$ -shifts become stronger, the relationship between source vs target performances becomes less consistent. In Appendix C.3, we also show that even for a fixed source distribution in one fixed prediction task, algorithmic rankings of performances on different target distributions vary a lot.

Tree ensemble methods show competitive performance, but do not significantly improve the generalization drop between source and target data. From Figure 5, tree-based ensembles (yellow bars) show robust and competitive performance on the target distribution in 6 out of 7 settings. However, in Figure 6 which plots the performance degradation between source and target, tree ensembles do not show improved robustness. This suggests that they do *not* actually achieve better robustness against real-world distribution shifts, and their better performances on

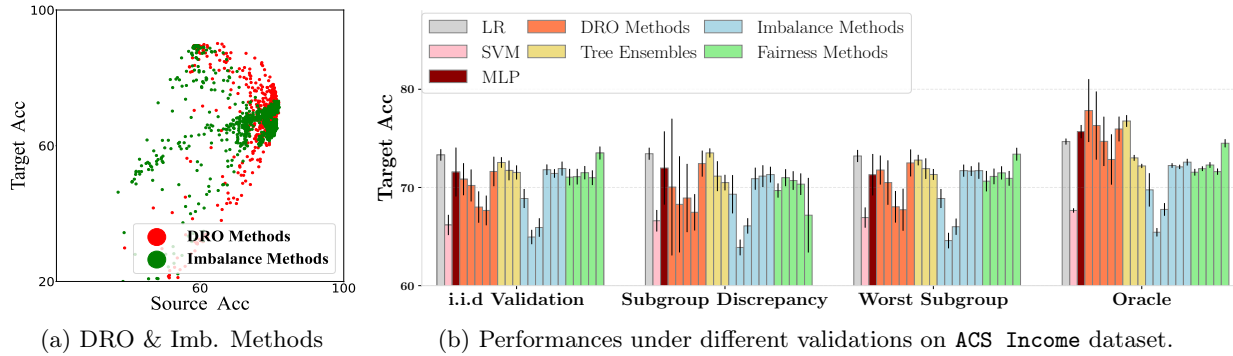


Figure 7. (a): Sensitivity of DRO methods and Imbalance Methods w.r.t. configurations. (b) Target performances of 22 algorithms under different validation protocols on ACS Income (CA→PR) setting.

target data may simply be due to better fitting the source distribution.

DRO methods are sensitive to configurations, with rankings varying significantly across 7 different settings. From Figure 5, DRO methods exhibit competitive performances on ACS Mobility (MS→HI), Taxi (NYC→BOG), and ACS Income (Young→Old), yet underperform in others. This sensitivity to configurations, as shown in Figure 7a (red points), could be attributed to the worst-case optimization that perturbs the training distribution within a pre-defined uncertainty set, without any information regarding the target distribution. However, when target information is incorporated for hyper-parameter tuning (as shown in Figure 7b), there is a marked improvement in the performance of DRO methods. Our observations suggest potential avenues for building more refined uncertainty sets in DRO methods.

Imbalance methods and fairness methods show similar performance with the base learner (XGBoost). In our experiments, we choose the XGBoost model as the base learner for imbalance and fairness methods due to its superior performance on tabular data [26]. However, from Figure 5 and Figure 6, imbalance methods and fairness methods do not show a clear improvement upon their base learner (XGBoost, last yellow bar). Further, as shown in Figure 7a, imbalance methods (green) are also quite sensitive to configurations, and their performances do not improve much when their hyperparameters are tuned over the target data (Oracle).

Target information matters in validation. Based on the ACS Income (CA→PR) dataset, we compare different validation protocols, including the best average accuracy, minimum subgroup discrepancy, and best worst-subgroup accuracy on validation data generated from the *source* distribution. We also use the Oracle validation that chooses the configuration with the best average accuracy on validation data generated from the *target* distribution. In Figure 7b, we find the first three protocols do not show a significant difference. However, oracle validation with target information substantially improves the effectiveness of both DRO and tree ensemble methods. We conclude using target information for model selection can provide robustness gains even with a small target dataset.

Non-algorithmic interventions warrant greater consideration. Reflecting on Section 3, it is clear that operational interventions yield significant enhancements for various methods, as demonstrated in Figure 4e and Figure 4f. In comparison to algorithmic interventions, such as designing different algorithms (e.g., DRO, Imbalance methods), a data-centric approach can be more effective in addressing distribution shifts. For instance, research on feature collection and feature engineering methods may prove impactful. Another avenue for future work is developing methods

that can optimally incorporate expensive samples from the target distribution.

5 Conclusion

We explore in depth the complexity of distribution shifts in real-world tabular datasets. Through a comprehensive case study, we demonstrate how a better understanding of distribution shifts facilitates algorithmic and data-based interventions. Using natural shifts from 5 real-world tabular datasets across different domains, we specify the shift pattern and evaluate 22 methods via experiments with over 86k trained models. Our benchmark WHYSHIFT encompasses various distribution shift patterns to evaluate the robustness of methods. Our findings highlight the importance of future research to understand how distributions differ in real-world applications.

Acknowledgement

We thank Tiffany Cai for her help with implementing the DISDE method on our benchmarks. Hongseok Namkoong was partially supported by the Amazon Research Award.

References

- [1] Us taxi dataset. <https://www.kaggle.com/competitions/nyc-taxi-trip-duration/data>, .
- [2] Other taxi dataset. <https://www.kaggle.com/datasets/mnavas/taxi-routes-for-mexico-city-and-quito>, .
- [3] R. Adragna, E. Creager, D. Madras, and R. S. Zemel. Fairness and robustness in invariant learning: A case study in toxicity classification. *CoRR*, abs/2011.06485, 2020. URL <https://arxiv.org/abs/2011.06485>.
- [4] A. Agarwal, A. Beygelzimer, M. Dudík, J. Langford, and H. Wallach. A reductions approach to fair classification. In *International Conference on Machine Learning*, pages 60–69. PMLR, 2018.
- [5] E. Amorim, M. Cançado, and A. Veloso. Automated essay scoring in the presence of biased ratings. In *Proceedings of the 2018 Conference of the North American Chapter of the Association for Computational Linguistics: Human Language Technologies, Volume 1 (Long Papers)*, pages 229–237, 2018.
- [6] S. Arakelyan, R. J. Das, Y. Mao, and X. Ren. Exploring distributional shifts in large language models for code analysis. *CoRR*, abs/2303.09128, 2023. doi: 10.48550/arXiv.2303.09128. URL <https://doi.org/10.48550/arXiv.2303.09128>.
- [7] M. Arjovsky, L. Bottou, I. Gulrajani, and D. Lopez-Paz. Invariant risk minimization. *arXiv preprint arXiv:1907.02893*, 2019.
- [8] P. Bandi, O. Geessink, Q. Manson, M. Van Dijk, M. Balkenhol, M. Hermsen, B. E. Bejnordi, B. Lee, K. Paeng, A. Zhong, et al. From detection of individual metastases to classification of lymph node status at the patient level: the camelyon17 challenge. *IEEE transactions on medical imaging*, 38(2):550–560, 2018.
- [9] R. K. E. Bellamy, K. Dey, M. Hind, S. C. Hoffman, S. Houde, K. Kannan, P. Lohia, J. Martino, S. Mehta, A. Mojsilovic, S. Nagar, K. N. Ramamurthy, J. T. Richards, D. Saha, P. Sattigeri, M. Singh, K. R. Varshney, and Y. Zhang. AI fairness 360: An extensible toolkit for detecting and mitigating algorithmic bias. *IBM J. Res. Dev.*, 63(4/5):4:1–4:15, 2019. doi: 10.1147/JRD.2019.2942287. URL <https://doi.org/10.1147/JRD.2019.2942287>.
- [10] S. Bird, M. Dudík, R. Edgar, B. Horn, R. Lutz, V. Milan, M. Sameki, H. Wallach, and K. Walker. Fairlearn: A toolkit for assessing and improving fairness in ai. *Microsoft, Tech. Rep. MSR-TR-2020-32*, 2020.
- [11] J. Blanchet, Y. Kang, and K. Murthy. Robust wasserstein profile inference and applications to machine learning. *Journal of Applied Probability*, 56(3):830–857, 2019.
- [12] K. Budhathoki, D. Janzing, P. Bloebaum, and H. Ng. Why did the distribution change? In *Proceedings of The 24th International Conference on Artificial Intelligence and Statistics*, pages 1666–1674. PMLR, 2021.
- [13] T. Cai, H. Namkoong, S. Yadlowsky, et al. Diagnosing model performance under distribution shift. *arXiv preprint arXiv:2303.02011*, 2023.

- [14] L. Cheng, R. Guo, R. Moraffah, P. Sheth, K. S. Candan, and H. Liu. Evaluation methods and measures for causal learning algorithms. *IEEE Transactions on Artificial Intelligence*, 3(6): 924–943, 2022.
- [15] E. Creager, J.-H. Jacobsen, and R. Zemel. Environment Inference for Invariant Learning. In *Proceedings of the 38th International Conference on Machine Learning*, pages 2189–2200. PMLR, 2021.
- [16] G. Csurka. A comprehensive survey on domain adaptation for visual applications. In G. Csurka, editor, *Domain Adaptation in Computer Vision Applications*, Advances in Computer Vision and Pattern Recognition, pages 1–35. Springer, 2017. doi: 10.1007/978-3-319-58347-1_1. URL https://doi.org/10.1007/978-3-319-58347-1_1.
- [17] P. Cui and S. Athey. Stable learning establishes some common ground between causal inference and machine learning. *Nat. Mach. Intell.*, 4(2):110–115, 2022. doi: 10.1038/s42256-022-00445-z. URL <https://doi.org/10.1038/s42256-022-00445-z>.
- [18] F. Ding, M. Hardt, J. Miller, and L. Schmidt. Retiring adult: New datasets for fair machine learning. *Advances in neural information processing systems*, 34:6478–6490, 2021.
- [19] D. Dua and C. Graff. UCI machine learning repository, 2017. URL <http://archive.ics.uci.edu/ml>.
- [20] J. Duchi, T. Hashimoto, and H. Namkoong. Distributionally robust losses for latent covariate mixtures. *Operations Research*, 71(2):649–664, 2023.
- [21] J. C. Duchi and H. Namkoong. Learning models with uniform performance via distributionally robust optimization. *The Annals of Statistics*, 49(3):1378–1406, 2021.
- [22] A. Farahani, S. Voghoei, K. Rasheed, and H. R. Arabnia. A brief review of domain adaptation. *CoRR*, abs/2010.03978, 2020. URL <https://arxiv.org/abs/2010.03978>.
- [23] J. Gardner, Z. Popović, and L. Schmidt. Subgroup Robustness Grows On Trees: An Empirical Baseline Investigation, 2022.
- [24] A. Ghorbani and J. Zou. Data shapley: Equitable valuation of data for machine learning. In *International Conference on Machine Learning*, pages 2242–2251. PMLR, 2019.
- [25] A. Ghorbani, J. Zou, and A. Esteva. Data shapley valuation for efficient batch active learning. In *2022 56th Asilomar Conference on Signals, Systems, and Computers*, pages 1456–1462. IEEE, 2022.
- [26] L. Grinsztajn, E. Oyallon, and G. Varoquaux. Why do tree-based models still outperform deep learning on tabular data?, 2022.
- [27] N. Haghtalab, M. Jordan, and E. Zhao. On-demand sampling: Learning optimally from multiple distributions. *Advances in Neural Information Processing Systems*, 35:406–419, 2022.
- [28] D. J. Hand. Classifier technology and the illusion of progress. *Statistical Science*, 2006.

- [29] M. Hardt, E. Price, and N. Srebro. Equality of opportunity in supervised learning. *Advances in neural information processing systems*, 29, 2016.
- [30] D. Hendrycks, S. Basart, N. Mu, S. Kadavath, F. Wang, E. Dorundo, R. Desai, T. Zhu, S. Parajuli, M. Guo, D. Song, J. Steinhardt, and J. Gilmer. The Many Faces of Robustness: A Critical Analysis of Out-of-Distribution Generalization, 2021.
- [31] M. A. Hernán, S. Hernández-Díaz, and J. M. Robins. A structural approach to selection bias. *Epidemiology*, pages 615–625, 2004.
- [32] W. Hu, G. Niu, I. Sato, and M. Sugiyama. Does Distributionally Robust Supervised Learning Give Robust Classifiers? In *Proceedings of the 35th International Conference on Machine Learning*, pages 2029–2037. PMLR, 2018.
- [33] B. Y. Idrissi, M. Arjovsky, M. Pezeshki, and D. Lopez-Paz. Simple data balancing achieves competitive worst-group-accuracy. In *Proceedings of the First Conference on Causal Learning and Reasoning*, pages 336–351. PMLR, 2022.
- [34] R. Jia, D. Dao, B. Wang, F. A. Hubis, N. Hynes, N. M. Gürel, B. Li, C. Zhang, D. Song, and C. J. Spanos. Towards efficient data valuation based on the shapley value. In *The 22nd International Conference on Artificial Intelligence and Statistics*, pages 1167–1176. PMLR, 2019.
- [35] A. E. Johnson, T. J. Pollard, L. Shen, L.-w. H. Lehman, M. Feng, M. Ghassemi, B. Moody, P. Szolovits, L. Anthony Celi, and R. G. Mark. Mimic-iii, a freely accessible critical care database. *Scientific data*, 3(1):1–9, 2016.
- [36] J. Kaddour, A. Lynch, Q. Liu, M. J. Kusner, and R. Silva. Causal machine learning: A survey and open problems. *arXiv preprint arXiv:2206.15475*, 2022.
- [37] P. W. Koh, S. Sagawa, H. Marklund, S. M. Xie, M. Zhang, A. Balsubramani, W. Hu, M. Yasunaga, R. L. Phillips, I. Gao, T. Lee, E. David, I. Stavness, W. Guo, B. Earnshaw, I. Haque, S. M. Beery, J. Leskovec, A. Kundaje, E. Pierson, S. Levine, C. Finn, and P. Liang. WILDS: A Benchmark of in-the-Wild Distribution Shifts. In *Proceedings of the 38th International Conference on Machine Learning*, pages 5637–5664. PMLR, 2021.
- [38] K. Kuang, R. Xiong, P. Cui, S. Athey, and B. Li. Stable prediction with model misspecification and agnostic distribution shift. In *Proceedings of the AAAI Conference on Artificial Intelligence*, volume 34, pages 4485–4492, 2020.
- [39] D. Levy, Y. Carmon, J. C. Duchi, and A. Sidford. Large-scale methods for distributionally robust optimization. *Advances in Neural Information Processing Systems*, 33:8847–8860, 2020.
- [40] R. Liaw, E. Liang, R. Nishihara, P. Moritz, J. E. Gonzalez, and I. Stoica. Tune: A research platform for distributed model selection and training. *arXiv preprint arXiv:1807.05118*, 2018.
- [41] J. Lim, C. X. Ji, M. Oberst, S. Blecker, L. Horwitz, and D. Sontag. Finding Regions of Heterogeneity in Decision-Making via Expected Conditional Covariance. <https://arxiv.org/abs/2110.14508v1>, 2021.

- [42] E. Z. Liu, B. Haghgoo, A. S. Chen, A. Raghunathan, P. W. Koh, S. Sagawa, P. Liang, and C. Finn. Just Train Twice: Improving Group Robustness without Training Group Information. In *Proceedings of the 38th International Conference on Machine Learning*, pages 6781–6792. PMLR, 2021.
- [43] Z. Liu, H. Ding, H. Zhong, W. Li, J. Dai, and C. He. Influence selection for active learning. In *2021 IEEE/CVF International Conference on Computer Vision, ICCV 2021, Montreal, QC, Canada, October 10-17, 2021*, pages 9254–9263. IEEE, 2021. doi: 10.1109/ICCV48922.2021.00914. URL <https://doi.org/10.1109/ICCV48922.2021.00914>.
- [44] S. M. Lundberg and S.-I. Lee. A unified approach to interpreting model predictions. *Advances in neural information processing systems*, 30, 2017.
- [45] S. M. Lundberg, G. Erion, H. Chen, A. DeGrave, J. M. Prutkin, B. Nair, R. Katz, J. Himmelfarb, N. Bansal, and S.-I. Lee. From local explanations to global understanding with explainable ai for trees. *Nature machine intelligence*, 2(1):56–67, 2020.
- [46] J. Miller, K. Krauth, B. Recht, and L. Schmidt. The effect of natural distribution shift on question answering models. In *International Conference on Machine Learning*, pages 6905–6916. PMLR, 2020.
- [47] J. P. Miller, R. Taori, A. Raghunathan, S. Sagawa, P. W. Koh, V. Shankar, P. Liang, Y. Carmon, and L. Schmidt. Accuracy on the Line: On the Strong Correlation Between Out-of-Distribution and In-Distribution Generalization. In *Proceedings of the 38th International Conference on Machine Learning*, pages 7721–7735. PMLR, 2021.
- [48] S. Moosavi, M. H. Samavatian, S. Parthasarathy, and R. Ramnath. A countrywide traffic accident dataset. *CoRR*, abs/1906.05409, 2019. URL <http://arxiv.org/abs/1906.05409>.
- [49] S. Moosavi, M. H. Samavatian, S. Parthasarathy, R. Teodorescu, and R. Ramnath. Accident risk prediction based on heterogeneous sparse data: New dataset and insights. In F. B. Kashani, G. Trajcevski, R. H. Güting, L. Kulik, and S. D. Newsam, editors, *Proceedings of the 27th ACM SIGSPATIAL International Conference on Advances in Geographic Information Systems, SIGSPATIAL 2019, Chicago, IL, USA, November 5-8, 2019*, pages 33–42. ACM, 2019. doi: 10.1145/3347146.3359078. URL <https://doi.org/10.1145/3347146.3359078>.
- [50] M. Oberst, F. D. Johansson, D. Wei, T. Gao, G. Brat, D. Sontag, and K. R. Varshney. Characterization of Overlap in Observational Studies, 2020.
- [51] S. J. Pan, I. W. Tsang, J. T. Kwok, and Q. Yang. Domain adaptation via transfer component analysis. In C. Boutilier, editor, *IJCAI 2009, Proceedings of the 21st International Joint Conference on Artificial Intelligence, Pasadena, California, USA, July 11-17, 2009*, pages 1187–1192, 2009. URL <http://ijcai.org/Proceedings/09/Papers/200.pdf>.
- [52] A. Paszke, S. Gross, F. Massa, A. Lerer, J. Bradbury, G. Chanan, T. Killeen, Z. Lin, N. Gimelshein, L. Antiga, A. Desmaison, A. Köpf, E. Z. Yang, Z. DeVito, M. Raison, A. Tejani, S. Chilamkurthy, B. Steiner, L. Fang, J. Bai, and S. Chintala. Pytorch: An imperative style, high-performance deep learning library. In H. M. Wallach, H. Larochelle, A. Beygelzimer, F. d’Alché-Buc, E. B. Fox, and R. Garnett, editors, *Advances in Neural Information Processing Systems 32*:

- Annual Conference on Neural Information Processing Systems 2019, NeurIPS 2019, December 8-14, 2019, Vancouver, BC, Canada*, pages 8024–8035, 2019. URL <https://proceedings.neurips.cc/paper/2019/hash/bdbca288fee7f92f2bfa9f7012727740-Abstract.html>.
- [53] F. Pedregosa, G. Varoquaux, A. Gramfort, V. Michel, B. Thirion, O. Grisel, M. Blondel, P. Prettenhofer, R. Weiss, V. Dubourg, J. VanderPlas, A. Passos, D. Cournapeau, M. Brucher, M. Perrot, and E. Duchesnay. Scikit-learn: Machine learning in python. *J. Mach. Learn. Res.*, 12:2825–2830, 2011. doi: 10.5555/1953048.2078195. URL <https://dl.acm.org/doi/10.5555/1953048.2078195>.
- [54] J. Peters, P. Bühlmann, and N. Meinshausen. Causal inference by using invariant prediction: identification and confidence intervals. *Journal of the Royal Statistical Society. Series B (Statistical Methodology)*, pages 947–1012, 2016.
- [55] B. Recht, R. Roelofs, L. Schmidt, and V. Shankar. Do imagenet classifiers generalize to imagenet? In *International conference on machine learning*, pages 5389–5400. PMLR, 2019.
- [56] M. Roberts, D. Driggs, M. Thorpe, J. Gilbey, M. Yeung, S. Ursprung, A. I. Aviles-Rivero, C. Etmann, C. McCague, L. Beer, et al. Common pitfalls and recommendations for using machine learning to detect and prognosticate for covid-19 using chest radiographs and ct scans. *Nature Machine Intelligence*, 3(3):199–217, 2021.
- [57] M. Rojas-Carulla, B. Schölkopf, R. E. Turner, and J. Peters. Invariant models for causal transfer learning. *J. Mach. Learn. Res.*, 19:36:1–36:34, 2018. URL <http://jmlr.org/papers/v19/16-432.html>.
- [58] S. Sagawa, P. W. Koh, T. B. Hashimoto, and P. Liang. Distributionally Robust Neural Networks for Group Shifts: On the Importance of Regularization for Worst-Case Generalization. *arXiv:1911.08731*, 2020.
- [59] R. Sahoo, L. Lei, and S. Wager. Learning from a biased sample. *arXiv preprint arXiv:2209.01754*, 2022.
- [60] S. Santurkar, D. Tsipras, and A. Madry. Breeds: Benchmarks for subpopulation shift. In *International Conference on Learning Representations*, 2021.
- [61] B. Schölkopf, D. Janzing, J. Peters, E. Sgouritsa, K. Zhang, and J. M. Mooij. On causal and anticausal learning. In *Proceedings of the 29th International Conference on Machine Learning, ICML 2012, Edinburgh, Scotland, UK, June 26 - July 1, 2012*. icml.cc / Omnipress, 2012. URL <http://icml.cc/2012/papers/625.pdf>.
- [62] B. Schölkopf, F. Locatello, S. Bauer, N. R. Ke, N. Kalchbrenner, A. Goyal, and Y. Bengio. Toward causal representation learning. *Proc. IEEE*, 109(5):612–634, 2021. doi: 10.1109/JPROC.2021.3058954. URL <https://doi.org/10.1109/JPROC.2021.3058954>.
- [63] S. Shafieezadeh-Abadeh, D. Kuhn, and P. M. Esfahani. Regularization via mass transportation. *Journal of Machine Learning Research*, 20(103):1–68, 2019.
- [64] V. Shankar, A. Dave, R. Roelofs, D. Ramanan, B. Recht, and L. Schmidt. Do image classifiers generalize across time? In *Proceedings of the IEEE/CVF International Conference on Computer Vision*, pages 9661–9669, 2021.

- [65] B. Sun, J. Feng, and K. Saenko. Return of frustratingly easy domain adaptation. In *Proceedings of the AAAI conference on artificial intelligence*, volume 30, 2016.
- [66] E. Tzeng, J. Hoffman, K. Saenko, and T. Darrell. Adversarial discriminative domain adaptation. In *Proceedings of the IEEE conference on computer vision and pattern recognition*, pages 7167–7176, 2017.
- [67] A. Wong, E. Otles, J. P. Donnelly, A. Krumm, J. McCullough, O. DeTroyer-Cooley, J. Pestrue, M. Phillips, J. Konye, C. Penozza, et al. External validation of a widely implemented proprietary sepsis prediction model in hospitalized patients. *JAMA Internal Medicine*, 181(8):1065–1070, 2021.
- [68] L. Wynants, B. Van Calster, G. S. Collins, R. D. Riley, G. Heinze, E. Schuit, E. Albu, B. Arshi, V. Bellou, M. M. Bonten, et al. Prediction models for diagnosis and prognosis of covid-19: systematic review and critical appraisal. *bmj*, 369, 2020.
- [69] B. Xie, L. Yuan, S. Li, C. H. Liu, and X. Cheng. Towards fewer annotations: Active learning via region impurity and prediction uncertainty for domain adaptive semantic segmentation. In *IEEE/CVF Conference on Computer Vision and Pattern Recognition, CVPR 2022, New Orleans, LA, USA, June 18-24, 2022*, pages 8058–8068. IEEE, 2022. doi: 10.1109/CVPR52688.2022.00790. URL <https://doi.org/10.1109/CVPR52688.2022.00790>.
- [70] Y. Yang, H. Zhang, D. Katabi, and M. Ghassemi. Change is hard: A closer look at subpopulation shift. *CoRR*, abs/2302.12254, 2023. doi: 10.48550/arXiv.2302.12254. URL <https://doi.org/10.48550/arXiv.2302.12254>.
- [71] Y. Yang, H. Zhang, D. Katabi, and M. Ghassemi. Change is Hard: A Closer Look at Subpopulation Shift, 2023.
- [72] H. Yao, C. Choi, B. Cao, Y. Lee, P. W. W. Koh, and C. Finn. Wild-time: A benchmark of in-the-wild distribution shift over time. *Advances in Neural Information Processing Systems*, 35: 10309–10324, 2022.
- [73] H. Yu, P. Cui, Y. He, Z. Shen, Y. Lin, R. Xu, and X. Zhang. Stable learning via sparse variable independence. *AAAI*, abs/2212.00992, 2022. doi: 10.48550/arXiv.2212.00992. URL <https://doi.org/10.48550/arXiv.2212.00992>.
- [74] J. R. Zech, M. A. Badgeley, M. Liu, A. B. Costa, J. J. Titano, and E. K. Oermann. Variable generalization performance of a deep learning model to detect pneumonia in chest radiographs: a cross-sectional study. *PLoS medicine*, 15(11):e1002683, 2018.
- [75] R. Zemel, Y. Wu, K. Swersky, T. Pitassi, and C. Dwork. Learning fair representations. In *International conference on machine learning*, pages 325–333. PMLR, 2013.
- [76] R. Zhai, C. Dan, Z. Kolter, and P. Ravikumar. DORO: Distributional and Outlier Robust Optimization. In *Proceedings of the 38th International Conference on Machine Learning*, pages 12345–12355. PMLR, 2021.
- [77] H. Zhang, H. Singh, M. Ghassemi, and S. Joshi. "Why did the Model Fail?": Attributing Model Performance Changes to Distribution Shifts, 2023.

- [78] X. Zhang, Y. He, T. Wang, J. Qi, H. Yu, Z. Wang, J. Peng, R. Xu, Z. Shen, Y. Niu, et al. Nico challenge: Out-of-distribution generalization for image recognition challenges. In *Computer Vision–ECCV 2022 Workshops: Tel Aviv, Israel, October 23–27, 2022, Proceedings, Part VI*, pages 433–450. Springer, 2023.

Appendices

A	Relevant Work and Some Comments	21
B	Case Study Details	23
B.1	Prevalence of $Y X$ -Shifts	23
B.2	Analysis of Decision Tree	23
B.3	Details of Non-algorithmic Interventions	24
B.4	Potential Alternative Approach of Identifying Risk Region	25
C	Benchmark Details	26
C.1	Datasets & Settings	26
C.2	Algorithms & Implementations	28
C.3	Parameter Search Space	29
C.4	Training Details	31
C.5	Detailed Results of 7 Selected Settings in Main Body	31
C.6	Full Results of 22 Settings	32
C.7	Worst-Domain Accuracy	33
C.8	Average Macro-F1 Score	33
C.9	Worst-Domain Macro-F1 Score	38
C.10	Agreement and Maintenance Plan	38

A Relevant Work and Some Comments

Distribution Shift Benchmarks. Existing distribution shift benchmarks primarily concentrate on image and language datasets [55, 37, 78, 60, 72] to assess the robustness and efficiency of algorithms in real applications. However, there is a noticeable lack of benchmark papers that specifically address real-world tabular datasets. These tabular datasets often present distinct patterns compared to image datasets, including prevalent methods [26] and shift patterns.

Therefore, it is important to understand detailed distribution patterns among these datasets to develop corresponding methodologies to address specific shifts, which is also observed in a recent benchmark [72]. Yang *et al.* [71] recently introduce one benchmark characterizing different patterns of subpopulation shift. This benchmark focuses on the relationship between a specific attribute and covariates, such as spurious correlation, which can be challenging to identify in tabular datasets. Besides, they focus on changes in the subpopulation, which is a subset of distribution shift patterns. For example, individuals in different states may suffer from little subpopulation shifts but still incur a large distribution shift. Individuals’ demographic features are similar but the income level differs greatly between CA and PR in `ACS Income`, as demonstrated in Table 2. Motivated by the challenges above, our work hopes to fill in the gap by demonstrating one benchmark on tabular datasets with detailed analysis.

Identifying Distribution Shifts on Features and Regions. Due to several model performance degradation in practice, machine learning communities are motivated to develop tools to explain the variation of model performance.

Table 2: Descriptive Characteristics under different states in ACS income dataset

State	CA	MA	NY	NE	MT	SD	PR
Total Size	195665	40114	103021	10785	5463	4899	9071
White Man	0.3311	0.4161	0.3687	0.4822	0.4959	0.4691	0.3526
Nonwhite Man	0.1969	0.0878	0.1379	0.0454	0.0428	0.0492	0.1818
White Woman	0.2873	0.4066	0.3464	0.4318	0.4221	0.4297	0.3124
NonWhite Woman	0.1847	0.0895	0.1471	0.0404	0.0392	0.0521	0.1532
$P(Y = 0)$	0.589	0.532	0.585	0.688	0.707	0.730	0.894

Among them, one common tool is the Shapley value [44, 45], which attributes model degradation to different components of the dataset. Shapley value can help evaluate how the variation of the prediction is attributed to each individual feature and conditional relationship [12, 77], i.e. decompose the shift on the joint distribution to particular X_i -shifts or the condition $X_j|X_i$ -shifts (X_i and X_j denote different features) under a known causal graph. However, existing Shapley value methods cannot quantify the effects of the joint shift to specific meaningful covariate regions in our case study. This means that the traditional Shapley value is not applicable to provide interventions in order for a better active learning procedure for specific samples. Some recent works extend the concept of Shapley value [24, 34, 25] to quantify the value of each data point to involve more relevant samples. It would be interesting to customize their data valuation tools to help understand the distribution shift better efficiently. Similar to our setup, Oberst *et al.* [50] and Lim *et al.* [41] developed specific methods to identify specific covariate regions where model learners are different. The difference between their setup and ours lies in the sampling and assumption of observed data. In their approach, the observed data is sampled i.i.d. across various prediction models, without any distribution shift. Besides, they can observe only one selected prediction result per sample from all the model learners. However, in our case study, the models are built on datasets from two domains that experience distribution shifts. As a result, we can further isolate the model difference based on the shared input space X and differentiate it from the total difference, specifically focusing on the $Y|X$ -shifts.

Choice of Domains in Distribution Shifts Although it is popular in the fairness literature to use the adult and ACS dataset with each demographic subgroup as one domain [75, 15, 18], the *relative regret* of models trained on these domains is quite small shown in Figure 1 empirically. This implicitly shows that $Y|X$ -shifts are not strong across different demographic subgroups. In contrast, the model usually experiences relatively large $Y|X$ -shifts under different spatial domains, which corresponds to the right-hand side of Figure 1. Besides, from the practical perspective, machine learning models often need to be deployed in spatial domains (city, state, and country-wise) only with few observed data while the model is trained with abundant data from the source domain. This is why we mainly choose spatial/temporal domains to benchmark distribution shifts in our case.

Limitations. We acknowledge some limitations of our benchmark. First, we only consider the source-target transfer pairs from datasets including the economic and transportation domain, and we leave the detailed pattern evaluation of these datasets in other domains such as the medical area (e.g. MIMIC-III [35]) as an interesting direction of the future work. Besides, we only consider the source and target from one fixed domain (i.e. one state or city). In practice, it is reasonable to

extend this benchmark to consider the source and the target distribution with multiple domains with varying proportions. And our results of characterizing the distribution shift patterns highlight the importance of utilizing other refined tools. These tools can help us understand the difference between real-world distribution shifts and enable further investigation and analysis.

B Case Study Details

In this section, we provide more details about our case study in the main body.

B.1 Prevalence of $Y|X$ -Shifts

For each of the 7 settings in Table 1, we only select one target distribution in the main body, while our benchmark supports multiple target distributions. Specifically, for **ACS Income**, **ACS Mobility**, **ACS Pub.Cov**, we have 50 target distributions (the other 50 American states) in total for each setting; for **Taxi**, we have 3 target distributions (other cities Mexico City, Bogotá, Quito); for the temporal shift version of **ACS Pub.Cov** (i.e. setting 6), we have 3 target distributions (i.e. the year 2014, 2017, and 2021); and for **US Accident**, we have 13 target distributions (13 American states). Therefore, we have an extension of 169 source-target transfer pairs in total for these 7 settings.

We use XGBoost classifier and calculate the decomposition of performance degradation via DISDE [13]. We calculate the **$Y|X$ -shift ratio** from the source distribution P to the target distribution Q following notations in [13]:

$$Y|X\text{-shift ratio} = \frac{\mathbb{E}_{S_X}[R_Q(X) - R_P(X)]}{\mathbb{E}_Q[\ell(f(X), Y)] - \mathbb{E}_P[\ell(f(X), Y)]},$$

where $R_\mu(x) := \mathbb{E}_\mu[\ell(f(X), Y)|X = x]$ for $\mu = P, Q$ denotes the conditional risk for each data distribution and S_X is the shared distribution over X whose support is contained in that of P_X and Q_X . We first focus on pairs with relatively strong distribution shifts (i.e. performance degradation larger than 8 percentage points). Across these pairs, we find that **70.2%** pairs have over **60%** $Y|X$ -shifts, and **87.2%** pairs have over **50%** $Y|X$ -shifts, indicating the prevalence of $Y|X$ shifts. To visualize the result better, in all 22 settings in our benchmark (as shown in Table 3), we focus on transfer pairs with performance degradation larger than 5 percentage points and plot the histogram of the ratio of $Y|X$ -shifts in Figure 8. From Figure 8, we could see that $Y|X$ -shifts are prevalent in real-world distribution shifts.

B.2 Analysis of Decision Tree

In Algorithm 1, we use a shallow *decision tree* $h(x)$ to approximate $y = |f_P(x) - f_Q(x)|$ on the shared distribution S_X to find the covariate region with highest discrepancy. In our decision tree, we use the *squared error* as the splitting criterion. And below we demonstrate that this criterion is equivalent to maximizing the discrepancy between two children nodes.

Suppose there are N samples with outcomes $\{y_i\}_{i \in [N]}$ belonging to tree node fa , and these samples are split into two children nodes s_1, s_2 , where the node s_1, s_2 denote the set of sample indices in the two children nodes respectively. The squared error criterion to split fa into s_1 and s_2 is:

$$\min_{s_1, s_2} \left\{ \mathcal{L}(s_1, s_2) := \frac{1}{N} \left(\sum_{i \in s_1} (y_i - \mu_{Y,1})^2 + \sum_{i \in s_2} (y_i - \mu_{Y,2})^2 \right) \right\}, \quad (\text{B.1})$$

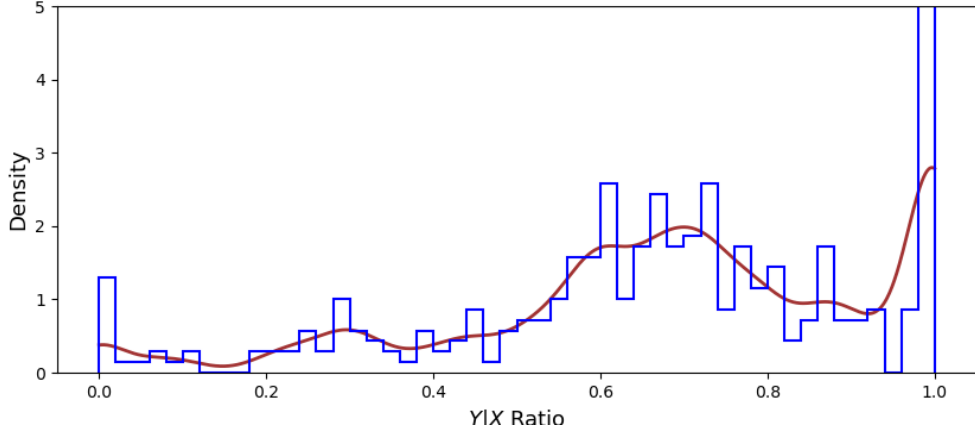


Figure 8: Histogram of $Y|X$ -shift ratio in our benchmark.

where

$$\mu_{Y,1} := \frac{\sum_{i=1}^N y_i \mathbf{1}_{\{i \in s_1\}}}{\sum_{i=1}^N \mathbf{1}_{\{i \in s_1\}}}, \quad \mu_{Y,2} := \frac{\sum_{i=1}^N y_i \mathbf{1}_{\{i \in s_2\}}}{\sum_{i=1}^N \mathbf{1}_{\{i \in s_2\}}} \quad (\text{B.2})$$

denote the mean values of the outcome Y with samples in children nodes s_1 and s_2 . Denote the distribution of the outcome Y follows the empirical distribution over the N samples $\{y_i\}_{i \in [N]}$. Simplifying (B.1), we have:

$$\mathcal{L}(s_1, s_2) = P(Y \in s_1) \text{Var}_{s_1}(Y) + P(Y \in s_2) \text{Var}_{s_2}(Y) = \mathbb{E}_S[\text{Var}(Y|S)], \quad (\text{B.3})$$

where $\text{Var}_s(Y)$ denotes the variance of the outcome variable Y in node s , $S = \{s_1, s_2\}$ is the variable representing the children nodes. Therefore, given that $\text{Var}_{f_a}(Y) := \text{Var}_S(\mathbb{E}[Y|S]) + \mathbb{E}_S[\text{Var}(Y|S)]$ is constant, the minimal $\mathbb{E}_S[\text{Var}(Y|S)]$ corresponds with the largest $\text{Var}_S(\mathbb{E}[Y|S])$, which maximizes the discrepancy of the outcome between two children nodes.

B.3 Details of Non-algorithmic Interventions

In Section 3.2, we propose two potential non-algorithmic interventions to mitigate the performance degradation. In this section, we introduce in detail the intervention of collecting specific data from the target.

Experiment Setup We focus on the income prediction task using the **ACS Income** dataset. Consider a practical scenario where the training set consists of 20,000 samples from California (CA) and the trained model was deployed in Puerto Rico (PR) in trial. After the trial deployment in PR, we got a *small amount* of samples from PR with labels and observed performance degradation. Under this setting, we investigate the effect of non-algorithmic interventions.

Collect specific data from the target We first identify the regions with high discrepancy between source and target. Note that the sample size of the target state is small compared to the training samples. Then for typical algorithms like logistic regression (LR), MLP, random forest (RF), LightGBM and XGBoost, we compare the performances of:

- original setting (only 20,000 samples from the source);
- original setting with N additional random samples drawn from the whole target state;
- original setting with N additional random samples drawn from the *risk region* of the target state.

In this experiment, we first select the best configuration of each method according to the *i.i.d* validation set in the original setting (only samples from CA), and fix it for the other two interventions. We vary N as 100, 200, 300 and the results are shown in Figure 9. From Figure 9, incorporating data from the risk region leads to a *stable improvement* on typical algorithms even for small target sample sizes. However, we observe that LightGBM and XGBoost would easily overfit f_Q on the target data, and we use random forest under this setup as an alternative. It is worth investigating approaches to find risk regions effectively under small/imbalanced sample sizes in the future. The approach mentioned here is a simple way of non-algorithmic and explainable interventions and we hope it could inspire further research in this direction.

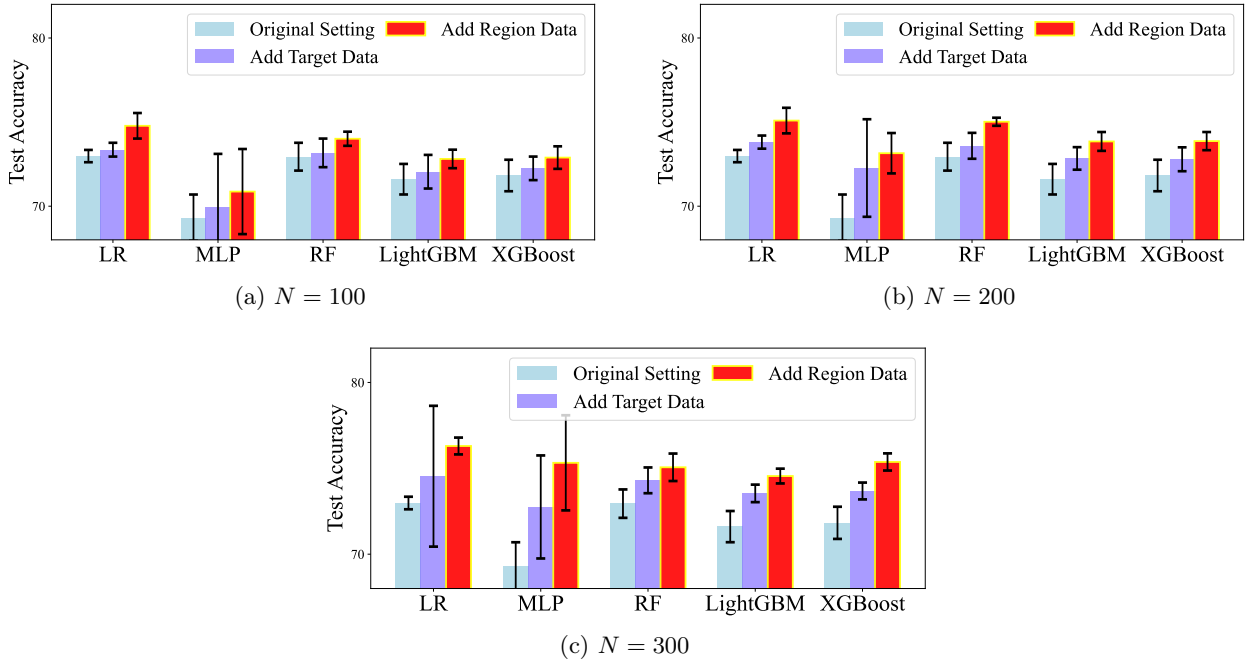


Figure 9: Test accuracies of different ways to incorporate data.

B.4 Potential Alternative Approach of Identifying Risk Region

In Algorithm 1, we propose a simple way to identify the risk region to explain the cause of $Y|X$ -shifts. And the identified region could be used to guide the collecting process of target data, which could help to further reduce the effects of performance degradation. However, in practice, when the amount of target samples is quite small, it may be hard to train the f_Q only with target samples accurately. Therefore, it may be better to propose a method that does not need f_Q to fit $Q(Y|X)$ on the target distribution.

Following this idea, we propose an alternative way of Algorithm 1. Since the training data is

enough, it is feasible to fit f_P on the shared distribution S_X as:

$$f_P := \operatorname{argmin}_{f \in \mathcal{F}} \mathbb{E}_P \left[\frac{dS_X}{dP_X} \ell(f(X), Y) \right]. \tag{B.4}$$

Then for n_Q samples from target distribution Q , we could use a prediction model $h(x)$ to approximate $|Y - f_P(X)|$ on the shared distribution (by reweighting density ratio $\frac{dS_X}{dQ_X}$). Note that this method does not need to train f_Q on target samples, but the quality of the density ratio dS_X/dP_X and the prediction model $h(x)$ still depend on the target samples. We hope the estimation of the ratio and the residuals $|Y - f_P(X)|$ can be less affected by the low sample size n_Q . This non-algorithmic intervention is not the main focus of this work, but we hope this idea could help to promote this line of research.

C Benchmark Details

In this section, we provide the details of our benchmark. In our benchmark, we explore distribution shifts on 5 real-world tabular datasets from the economic and traffic sectors with natural spatial or temporal distribution shifts. We carefully design 22 settings utilizing these 5 datasets, and the overview of 22 settings is shown in Table 3. Note that in our main body, due to space limitations, we only pick 7 typical settings and select only one representative target domain for each setting, as shown in Table 1. Detailed introductions of all datasets, algorithms, and experiment settings will be given in the following sections. A Python package for our benchmark can be found at <https://github.com/namkoong-lab/whyshift>.

C.1 Datasets & Settings

Here we introduce 5 real-world tabular datasets in detail. **ACS Income**, **ACS Mobility**, **ACS Public Coverage** are based on the American Community Survey (ACS) Public Use Microdata Sample (PUMS) [18]. And here we use the same data filtering as [18].

ACS Income The task is to predict whether an individual’s income is above \$50,000. We filter the dataset to only include individuals above the age of 16, usual working hours of at least 1 hour per week in the past year, and an income of at least \$100.

- In our Setting 1~4, we use data from 2018 and the source/target domain refers to American states, which contain natural spatial distribution shifts. We train methods on data from California, Connecticut, Massachusetts, and South Dakota respectively, and test the generalization performance on the other 50 American states.
- In our Setting 21~22, we sub-sample the dataset according to age to introduce covariate shift, where we focus on individuals from California and form two groups according to whether their age is ≥ 25 . In Setting 21, the source data over-samples the low age group where 80% is drawn from the age ≥ 25 group, and the proportions are reversed in the target data (20% from age ≥ 25 group). In Setting 22, the source data over-samples the low age group where 90% is drawn from the age ≥ 25 group, and the proportions are reversed in the target data (10% from age ≥ 25 group).

Table 3. Overview of datasets and the whole 22 selected settings. In our benchmark, each setting has multiple target domains (except the last setting). In our main body, we select only one target domain for each setting. \diamond : we report the ‘‘Dom. Ratio’’ to represent the dominant ratio of $Y|X$ shifts or X shifts in source-target pairs with performance degradation larger than 5 percentage points in each setting. For example, ‘‘ $Y|X: 13/14$ ’’ means that there are 14 source-target pairs in Setting 1 with degradation larger than 5 percentage points and 13 out of them with over 50% degradation attributed to $Y|X$ shifts. We use XGBoost to measure this.

#ID	Dataset	Type	#Features	Outcome	Source	#Train Samples	#Test Domains	Dom. Ratio \diamond
1	ACS Income	Spatial	9	Income \geq 50k	California	195,665	50	$Y X: 13/14$
2	ACS Income	Spatial	9	Income \geq 50k	Connecticut	19,785	50	$Y X: 24/24$
3	ACS Income	Spatial	9	Income \geq 50k	Massachusetts	40,114	50	$Y X: 21/22$
4	ACS Income	Spatial	9	Income \geq 50k	South Dakota	4,899	50	$Y X: 9/9$
5	ACS Mobility	Spatial	21	Residential Address	Mississippi	5,318	50	$Y X: 28/34$
6	ACS Mobility	Spatial	21	Residential Address	New York	40,463	50	$Y X: 30/31$
7	ACS Mobility	Spatial	21	Residential Address	California	80,329	50	$Y X: 9/17$
8	ACS Mobility	Spatial	21	Residential Address	Pennsylvania	23,918	50	$Y X: 17/17$
9	Taxi	Spatial	7	Duration time \geq 30 min	Bogotá	3,063	3	$Y X: 1/2$
10	Taxi	Spatial	7	Duration time \geq 30 min	New York City	1,458,646	3	$Y X: 3/3$
11	ACS Pub.Cov	Spatial	18	Public Ins. Coverage	Nebraska	6,332	50	$Y X: 32/39$
12	ACS Pub.Cov	Spatial	18	Public Ins. Coverage	Florida	71,297	50	$Y X: 28/29$
13	ACS Pub.Cov	Spatial	18	Public Ins. Coverage	Texas	98,928	50	$Y X: 33/34$
14	ACS Pub.Cov	Spatial	18	Public Ins. Coverage	Indiana	24,330	50	$Y X: 11/13$
15	US Accident	Spatial	47	Severity of Accident	Texas	26,664	13	$Y X: 7/7$
16	US Accident	Spatial	47	Severity of Accident	California	64,909	13	$X: 22/31$
17	US Accident	Spatial	47	Severity of Accident	Florida	32,278	13	$X: 5/7$
18	US Accident	Spatial	47	Severity of Accident	Minnesota	8,927	13	$X: 8/11$
19	ACS Pub.Cov	Temporal	18	Public Ins. Coverage	Year 2010 (NY)	73,208	3	$X: 2/2$
20	ACS Pub.Cov	Temporal	18	Public Ins. Coverage	Year 2010 (CA)	149,441	3	$X: 2/2$
21	ACS Income	Synthetic	9	Income \geq 50k	Younger People (80%)	20,000	1	$X: 1/1$
22	ACS Income	Synthetic	9	Income \geq 50k	Younger People (90%)	20,000	1	$X: 1/1$

ACS Mobility The task is to predict whether an individual had the same residential address one year ago. We filter the dataset to only include individuals between the ages of 18 and 35, which increases the difficulty of the prediction task.

- In our Setting 5~8, we use data from 2018 and the source/target domain refers to American states, which contain natural spatial distribution shifts. We train methods on data from Mississippi, New York, California, and Pennsylvania respectively, and test the generalization performance on the other 50 American states.

ACS Public Coverage The task is to predict whether an individual has public health insurance. We focus on low-income individuals who are not eligible for Medicare by filtering the dataset to only include individuals under the age of 65 and with an income of less than \$30,000.

- In our Setting 11~14, we use data from 2018 and the source/target domain refers to American states, which contain natural spatial distribution shifts. We train methods on data from Nebraska, Florida, Texas, and Indiana respectively, and test the generalization performance on the other 50 American states.
- In our Setting 19~20, we consider the temporal shifts. We use data from 2010 in training and data from 2014, 2017, and 2021 in testing (3 test domains). In Setting 19, the training data come from New York, and in Setting 20, the training data come from California.

US Accident The task is to predict whether an accident is severe (long delay) or not (short delay) based on weather features and Road conditions features.

- In our Setting 15~18, the source/target domain refers to American states, which contain natural spatial distribution shifts. We train methods on data from California, Florida, Texas, and Minnesota respectively, and test the generalization performance on other 13 American states. Here we only involve 13 test domains because the sample sizes in the other states are quite small.

Taxi The task is to predict whether the total ride duration time exceeds 30 minutes, based on location and temporal features. We filter the data in 2017 and remove some extremely large or small features (e.g. samples with too long distances which can be easily classified).

- In our Setting 9~10, we use data from 2016 and the source/target domain refers to different cities. We train methods on data from Bogota and New York City and test the generalization performance in the other cities.

C.2 Algorithms & Implementations

In our benchmark, we evaluate 22 algorithms that span a wide range of learning strategies on tabular data and compare their performances under different patterns of distribution shifts we construct. Concretely, these algorithms include:

Base Methods We include some typical supervised learning methods for tabular data: Logistic Regression (LR), SVM, and fully-connected neural networks (MLP) with standard ERM optimization. For LR and SVM, we use the standard implementation in `scikit-learn` [53] and train them on CPUs. For MLP, we implement it via `PyTorch` [52] and train it on GPUs.

Tree Ensemble Models As shown by Gardner *et al.* [23], several tree-based methods achieve good performances on tabular datasets. And gradient-boosted trees (e.g., XGBoost, LightGBM) are widely considered as the state-of-the-art methods on tabular data. Therefore, we evaluate XGBoost and LightGBM in our benchmark. Also, we evaluate Random Forest (RF) to incorporate the performance of tree bagging methods.

DRO Methods Distributionally Robust Optimization (DRO) methods are proposed to address the distribution shifts, which is the form of:

$$\min_{\theta \in \Theta} \sup_{Q \in \mathcal{P}(P_{tr})} \mathbb{E}_Q[\ell(f_\theta(X), Y)], \tag{C.1}$$

where $\mathcal{P}(P_{tr})$ denotes the uncertainty set around the training distribution P_{tr} . Following Gardner *et al.* [23], we implement two typical variants of DRO, namely CVaR-DRO and χ^2 -DRO. CVaR-DRO is equivalent to Conditional Value at Risk (CVaR), and χ^2 -DRO uses χ^2 -divergence to regulate the uncertainty set. We use the fast implementation [39] in `PyTorch` [52]. We also consider the DORO [76], which discards a proportion ϵ of the largest error points in each iteration to mitigate the outliers in DRO with two variants, CVaR-DORO and χ^2 -DORO. We also evaluate the Group DRO [58], which is proposed to minimize the worst-group loss and shows good generalization performances

on many vision tasks. This method needs the group label and we define groups according to the “SEX” feature on ACS datasets. For US Accident and Taxi, we do not run Group DRO, since the current Group DRO model in the codebase only accepts the input with few groups while it is hard to define such group here. For all DRO methods, we use the MLP as the backbone model. We do not choose tree ensemble methods since tree ensemble methods are difficult to adapt to the distributionally robust case. Therefore, we leave their method developments and implementations as our future work.

Imbalanced Learning Methods Recently, some simple data balancing methods [33] have shown good worst-group performances under distribution shifts. In our benchmark, we implement 4 typical balancing methods, namely Sub-Sampling Y (SUBY), Reweighting Y (RWY), Sub-Sampling Group (SUBG), and Reweighting Group (RWG). Besides, “Just Train Twice” (JTT [42]) exhibits good performances in many vision tasks, and therefore we also evaluate it in our tabular settings. Furthermore, stable learning methods [38, 17] propose to de-correlate sample covariates for an accurate estimation of causal relationships via global balancing, which could mitigate distribution shifts. In our benchmark, we implement one typical method named DWR [38]. For these imbalanced learning methods, we use XGBoost as the backbone model due to its superiority on tabular data and adjust sample weight or training procedure accordingly for each of the methods.

Fairness-enhancing Methods Following Ding *et al.* [18] and Gardner *et al.* [23], fairness-enhancing methods have the potential to mitigate the performance degradation under distribution shifts. In our benchmark, we evaluate the in-processing and post-processing intervention methods. The in-processing method [4] minimizes the prediction error subject to some fairness constraints, and in our benchmark, we choose three typical fairness constraints, including demographic parity (DP), equal opportunity (EO), error parity (EP). And the post-processing method [29] randomizes the predictions of a fixed classifier to satisfy equalized odds criterion, and we use exponential and threshold controls in our benchmark. We use the implementations of `aif360` [9] and `fairlearn` [10].

C.3 Parameter Search Space

We provide the hyperparameter grids in Table 4. We mainly use the hyperparameter grids proposed in [23], and we restrict the grid size of each method in each setting to 200 in consideration of computational costs. For each setting, we randomly pick 200 configurations for each algorithm for a fair comparison. For methods incorporating backbone models (e.g., MLP/XGBoost), we choose the top 10 best configurations for that backbone model to reduce the search space, making the searched best configuration represent its best performance more accurately. Moreover, to accelerate the grid search process, we utilize Ray [40] to run experiments in parallel.

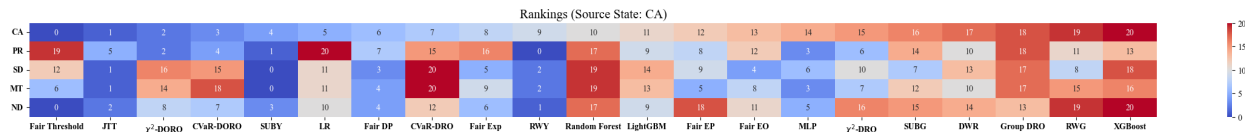


Figure 10. Algorithmic rankings vary across different target states for the fixed source state and task.

Table 4. Hyperparameter grids used in all experiments. \diamond : for methods with the total grid size above 200, we randomly sample 200 configurations for fair comparisons. For methods incorporating backbone models (e.g., MLP/XGBoost), we choose top-10 best configurations for that backbone model to reduce the search space, making the searched best configuration represent its best performance more accurately.

Model	Total Grid Size	Hyperparameter	Value Range
Base Methods			
MLP	270 \diamond	Learning Rate Batch Size Hidden Units Dropout Ratio Train Epoch	{0.001, 0.003, 0.0001, 0.005, 0.01} {64, 128, 256} {16, 32, 64} {0, 0.1} {50, 100, 200}
SVM	96	C Kernel Loss γ	{0.01, 0.1, 1, 10, 100, 1000} {linear, RBF} Squared Hinge {0.1, 0.3, 0.5, 1.0, 1.5, 2.0, scale, auto}
Logistic Regression	23	L_2 penalty	{0.001, 0.03, 0.005, 0.007, 0.01, 0.03, 0.05, ... 1.3, 1.7, 5, 10, 50, 100, 5e2, 1e3, 5e3, 1e4}
Tree Ensemble Methods			
Random Forest	640 \diamond	Num. Estimators Max Features Min. Samples Split Min. Samples Leaf Cost-Complexity α	{32, 64, 128, 256, 512} {sqrt, log2} {2, 4, 8, 16} {1, 2, 4, 8} {0., 0.001, 0.01, 0.1}
XGBoost	1944 \diamond	Learning Rate Min. Split Loss Max. Depth Column Subsample Ratio (tree) Column Subsample Ratio (level) Max. Bins Growth Policy	{0.1, 0.3, 1.0, 2.0} {0, 0.1, 0.5} {4, 6, 8} {0.7, 0.9, 1} {0.7, 0.9, 1} {128, 256, 512} {Depthwise, Loss Guide}
LightGBM	1680 \diamond	Learning Rate Num. Estimators L_2 -reg. Min. Child Samples Column Subsample Ratio (tree)	{0.01, 0.1, 0.5, 1.} {64, 128, 256, 512} {0., 0.001, 0.01, 0.1, 1.} {1, 2, 4, 8, 16, 32, 64} {0.5, 0.8, 1.}
DRO Methods			
DRO χ^2	1890 \diamond	Uncertainty set size α Backbone Model	{0.01, 0.1, 0.2, 0.3, 0.4, 0.5, 0.6} MLP
DRO CVaR	1890 \diamond	Uncertainty set size α Backbone Model	{0.001, 0.01, 0.1, 0.2, 0.3, 0.4, 0.5, 0.6} MLP
DORO χ^2	8100 \diamond	Uncertainty set size α Outlier proportion ϵ Backbone Model	{0.1, 0.2, 0.3, 0.4, 0.5, 0.6} {0.001, 0.01, 0.1, 0.2, 0.3} MLP
DORO CVaR	8100 \diamond	Uncertainty set size α Outlier proportion ϵ	{0.1, 0.2, 0.3, 0.4, 0.5, 0.6} {0.001, 0.01, 0.1, 0.2, 0.3}
Group DRO	1080 \diamond	Group weights step size Backbone Model	{0.001, 0.01, 0.1, 0.2} MLP
Imbalanced Learning Methods			
SUBY, RWY, SUBG, RWG	1944 \diamond	Backbone Model	XGBoost
JTT	11664 \diamond	Up-weight λ Backbone Model	{4, 5, 6, 20, 50, 100} XGBoost
DWR	48600 \diamond	L_1 penalty λ L_2 penalty λ Backbone Model	{1e-3, 1e-2, 1e-1, 0.2, 0.3} {1e-3, 1e-2, 1e-1, 0.2, 0.3} XGBoost
Fairness Methods			
In-processing	1944 \diamond	Constraint Type Backbone Model	{DP, EO, Error Parity} XGBoost
Post-processing	1944 \diamond	Constraint Type Backbone Model	{Exp, Threshold} XGBoost

C.4 Training Details

In each setting, we randomly sample 20,000 samples from the source domain for training, 20,000 samples from the source domain for validation, and 20,000 samples from the target domain for testing. For **US Accident** and **Taxi** datasets, we only randomly sample 8,000 samples for the source/target domain due to fewer samples involved in each setting. For setting where the source domain has fewer samples, we use 80% samples for training and 20% for validation. For results not specified by the validation protocol, we selected the best configuration according to the performance on such validation set (*i.i.d* with training).

For settings with **ACS Income**, **ACS Public Coverage**, **ACS Mobility** and **US Accident** datasets, all experiments were run on a server using 48 cores from two AMD EPYC 7402 24-Core Processors. For settings with **Taxi** dataset, all experiments were run on a cluster using 24 cores from an Intel Xeon Gold 6126 Processor. Neural-network-based models (MLP, DRO methods) were trained on GPU, NVIDIA GeForce RTX 3090, the other methods were trained only on CPUs. Note that all experiments are small-scale and could be run efficiently. Besides, during training, we found that the bi-search in χ^2 -DRO sometimes failed to converge, and therefore we set the maximal iteration num to 2500.

C.5 Detailed Results of 7 Selected Settings in Main Body

In the main body, due to space limitations, we only visualize the target performances of different methods. Here we provide the detailed results of all algorithms on the 7 selected settings in Table 1. We select the top-10 configurations according to the validation set *i.i.d* with training data and report the mean accuracy as well as the standard deviation in Table 5. Also, in Figure 11, we visualize the results of 22 algorithms of all configurations in our 7 selected settings.

Analysis From the numbers of numerical results in that Table, we give a more detailed analysis corresponding with our main body.

- Different algorithms do not exhibit consistent rankings over different distribution shift patterns. In Table 5, we boldface the best target performance within each class of methods. And we show the top-3 classes at the bottom. The results show that the algorithmic rankings across different settings and tasks are quite different. And even the rankings of algorithms within the same class vary a lot. This further demonstrates the complexity of $Y|X$ shifts. Also, Figure 10 shows that even for the fixed source state, algorithmic rankings vary a lot across different target states.
- Tree ensemble methods show competitive performances but do not significantly eliminate the generalization error between source and target data, characterized by the difference between *o.o.d.* and *i.i.d.* model performance. From the bottom, we could see that tree ensemble methods achieve top-3 performances in most of the selected settings (6 out of 7), exhibiting their superiority on tabular data. However, the performance degradation between source and target is still large.
- Imbalance methods and fairness methods show similar performance with the base learner (XGBoost). We find these methods do not have a significant improvement over the base learner (XGBoost). This may be due to that they are not designed to incorporate tree ensemble methods.

Table 5. Results of 7 selected settings in the main body, where we run each method with its best configuration 10 times and report their mean accuracies and standard deviations.

Dataset		ACS Income		ACS Mobility		US Taxi		ACS Pub.Cov		US Accident		ACS Time		Sub-Sampling	
Shift Pattern		Y X dominates		Y X dominates		Y X dominates		Y X more		Y X more		X more		X dominates	
Source → Target Pair		CA→PR		MS→HI		NYC→BOG		NE→LA		CA→OR		2010→2017		Young→Old	
		<i>i.d.</i>	<i>o.o.d</i>	<i>i.d.</i>	<i>o.o.d</i>	<i>i.d.</i>	<i>o.o.d</i>	<i>i.d.</i>	<i>o.o.d</i>	<i>i.d.</i>	<i>o.o.d</i>	<i>i.d.</i>	<i>o.o.d</i>	<i>i.d.</i>	<i>o.o.d</i>
Base Methods	LR	80.5±0.2	73.2±0.2	76.9 ±0.2	76.9 ±2.6	83.6±0.3	73.7±0.2	83.2±0.6	66.3±1.4	82.3±0.3	67.7±0.3	75.3±1.8	66.7±2.4	92.4±0.0	81.5±0.0
	SVM	79.0±0.3	67.0±0.9	78.6±0.6	76.9±0.3	83.4±0.2	74.9±0.6	83.9±0.4	64.9±1.2	81.3±0.8	65.5±0.4	75.4±0.9	67.4±0.9	91.9±0.1	79.5±0.7
	MLP	80.9±0.4	68.9±2.5	76.8 ±0.5	76.4 ±2.7	84.5±0.5	73.8±0.5	82.5±1.1	66.4±2.6	83.6±0.5	63.5±0.8	77.0±1.0	70.5±0.5	92.3±0.1	81.6±0.3
Tree Methods	Random forest	81.1±0.2	72.9±0.4	80.2 ±0.3	72.0 ±0.3	85.8±0.2	73.4±0.8	85.5±0.3	68.3±0.4	86.2±0.5	66.5±0.4	78.5±0.2	70.6±0.3	92.2±0.1	81.2±0.1
	LightGBM	81.2±0.2	71.4±0.5	79.5 ±0.3	71.3 ±0.8	86.4±0.4	72.7±0.8	85.7±0.4	70.0±0.4	86.6±0.4	65.4±0.4	79.1±0.3	71.8±0.3	93.0±0.0	82.4±0.0
	XGBoost	81.4±0.2	71.7±0.6	80.0 ±0.4	71.2 ±0.8	86.5±0.4	73.0±0.7	85.8±0.5	70.1±0.3	86.6±0.4	65.4±0.3	79.0±0.3	71.6±0.2	92.6±0.0	81.6±0.0
DRO Methods (base: MLP)	χ ² -DRO	80.7±0.2	73.2±2.2	76.3 ±0.3	78.4 ±0.2	84.8±0.4	73.0±1.1	80.6±0.6	60.9±1.7	83.3±0.4	64.0±0.8	70.5±12.6	64.2±7.6	92.1±0.2	81.2±0.5
	CVaR-DRO	80.9±0.2	71.7±1.7	76.4 ±0.5	78.3 ±0.4	85.4±0.4	73.8±0.8	79.5±4.0	61.7±1.7	84.1±0.3	64.8±0.7	75.6±1.6	67.5±2.7	92.3±0.1	81.4±0.3
	χ ² -DORO	77.2±6.2	71.0±10.2	76.3 ±0.4	78.6 ±0.0	84.6±0.4	73.6±0.7	80.6±0.4	59.4±0.0	83.5±0.4	64.5±0.8	71.2±0.3	64.5±0.3	91.9±0.3	80.6±1.2
	CVaR-DORO	78.8±0.6	72.4±4.2	76.4 ±0.4	78.6 ±0.1	85.2±0.3	74.3±0.4	83.7±0.5	66.9±0.9	83.4±2.4	63.9±1.0	77.6±0.3	70.7±0.4	92.0±0.2	81.0±0.6
Imbalanced Learning Methods (base: XGB)	Group DRO	80.7±0.3	71.9±3.4	75.5 ±0.4	78.5 ±0.2	N/A	N/A	80.3±7.3	65.8±3.6	N/A	N/A	74.4±7.1	68.3±4.0	92.3±0.1	81.6±0.2
	JTT	77.9±0.4	69.7±1.3	77.2 ±0.3	70.1 ±0.8	85.0±0.3	71.4±1.1	84.1±0.8	68.9±0.4	85.9±0.4	65.9±0.7	72.9±0.4	67.7±1.0	91.5±0.0	79.0±0.0
	SUBY	80.5±0.2	64.9±0.7	76.0 ±0.2	70.3 ±2.6	85.8±0.4	72.0±1.9	75.2±1.0	68.6±0.7	85.3±0.3	64.4±0.4	73.5±0.4	70.3±1.5	85.7±0.4	68.5±0.7
Fairness Methods (base: XGB)	RWY	80.9±0.2	65.9±0.6	75.9 ±0.4	68.5 ±1.3	86.2±0.5	73.1±1.1	82.1±0.7	69.7±0.5	86.1±0.4	65.3±0.6	74.7±0.5	71.3±0.6	90.6±0.0	78.5±0.0
	SUBG	81.2±0.3	70.9±0.6	79.1 ±0.2	71.1 ±0.6	85.3±0.3	71.4±1.2	85.1±0.5	70.2±0.4	86.4±0.4	65.2±0.4	78.8±0.3	71.4±0.3	92.4±0.1	81.2±0.3
	RWG	81.4±0.2	71.5±0.5	79.7 ±0.2	71.0 ±0.8	86.3±0.4	72.8±0.9	85.8±0.5	70.1±0.3	86.7±0.4	65.2±0.4	79.1±0.4	72.1±0.3	92.9±0.0	82.5±0.0
Fairness Methods (base: XGB)	DWR	81.3±0.2	71.3±0.6	78.2 ±0.4	69.8 ±0.8	83.5±0.5	71.2±1.2	85.8±0.4	69.8±0.4	86.7±0.4	65.4±0.4	79.0±0.3	72.0±0.3	92.5±0.0	81.2±0.0
	DP	80.8±0.3	70.4±0.6	79.5 ±0.3	71.3 ±0.8	86.3±0.4	72.0±1.0	85.2±0.5	70.2±0.5	86.3±0.4	65.6±0.5	79.0±0.3	71.8±0.2	92.7±0.0	81.6±0.0
	EO	81.3±0.2	71.2±0.6	79.3 ±0.3	71.4 ±1.0	86.4±0.3	72.8±1.2	85.8±0.4	70.2±0.4	86.4±0.5	65.4±0.5	79.0±0.3	71.8±0.2	92.7±0.0	81.5±0.0
	EP	81.3±0.2	71.4±0.5	79.6 ±0.3	70.9 ±0.9	85.7±0.4	71.7±1.4	86.0±0.2	70.1±0.5	86.3±0.4	66.1±0.8	79.0±0.3	71.8±0.2	92.6±0.0	81.5±0.0
Fairness Methods (base: XGB)	Exp	80.9±0.2	70.6±0.6	79.4 ±0.6	71.2 ±0.9	85.6±0.5	71.5±1.1	85.5±0.2	70.2±0.5	85.8±0.4	65.5±0.6	79.0±0.3	71.8±0.2	92.6±0.0	81.5±0.0
	Threshold	77.2±0.3	73.6±0.4	77.5 ±0.5	69.9 ±1.3	84.1±0.6	54.3±0.4	84.5±0.3	68.2±0.7	83.8±0.5	64.5±0.6	78.8±0.2	71.7±0.3	91.6±0.0	78.3±0.0
Top 3 Classes		Fair>Base≈Rob.		DRO>Base≫Tree.		Base>DRO>Tree		Tree≈Fair≈Imb.		Base>Tree>Fair		Imb>Fair≈Tree		Tree≈Imb>Others	

C.6 Full Results of 22 Settings

In this section, we provide the full results of our 22 settings in Table 3.

C.6.1 Average Accuracy

In Table 6, Table 7 and Table 8, we report the source accuracy and the target accuracy of all algorithms. Since in these settings, we have multiple target domains, as for the target accuracy of each algorithm, we report the average accuracy as well as the standard deviation calculated on all target domains. Here the standard deviation reflects the stability of out-of-distribution generalization performances across different target domains instead of random seeds.

From the average result over, Table 6, Table 7 and Table 8, we can still obtain similar findings compared to that from the 7 selected settings in the main body. Especially, while tree ensemble methods serve as a strong in-sample benchmark illustrated by their competitive *i.i.d.* performance, these methods do not yield better performance than other methods in the target distribution uniformly. And when we average across different target domains, DRO methods do not perform better than their empirical counterpart, indicating that the worst-case optimization from the uncertainty sets constructed by existing DRO methods can rarely occur in practical setups and does not help much compared with standard ERM cases. This tricky part of worst-case intervention also holds when we compare imbalanced learning and fairness methods with the XGB base learner. These methods can lead to better *o.o.d.* results than the base learner sometimes indeed, while this may not hold true when we average over different target domains. In general, existing methods cannot generalize well averaging over different target domains, and it would be interesting to develop methods to close that gap.

Table 6. Average target domain accuracy of all algorithms on the ACS Income and ACS Pub.Cov datasets. In each setting, we test all algorithms on the 50 American states and report the mean and standard deviation across all 50 target states. The standard deviation here reflects the stability of performances across different target states.

Dataset		ACS INCOME								ACS PUB.COV							
Source State		CA		CT		MA		SD		FL		TX		NE		IN	
		<i>i.d.</i>	<i>o.o.d.</i>														
Base Methods	LR	81.1	77.3 ±1.9	80.7	76.2 ±2.3	80.9	76.8 ±2.2	80.1	75.8 ±3.3	81.3	73.7 ±7.3	84.1	73.9 ±7.2	84.3	75.0 ±6.7	78.6	75.8 ±5.9
	SVM	79.4	74.8 ±1.9	78.6	72.4 ±2.9	80.1	73.0 ±2.7	79.3	73.3 ±3.8	80.5	74.4 ±6.3	84.2	74.1 ±6.9	84.8	73.8 ±6.5	77.1	74.3 ±5.1
	MLP	81.8	76.4 ±2.6	81.4	76.8 ±2.3	81.7	77.4 ±2.2	80.5	76.8 ±2.9	83.3	76.5 ±6.4	85.4	76.6 ±6.5	84.5	75.3 ±6.3	78.8	76.2 ±5.9
Tree	Random Forest	81.7	77.9 ±1.8	81.2	77.1 ±2.1	81.5	77.4 ±2.0	80.2	75.5 ±3.6	84.6	77.3 ±6.7	86.8	77.0 ±6.8	86.7	76.2 ±6.7	81.2	77.7 ±5.4
Ensemble Methods	LightGBM	81.8	77.3 ±2.1	82.1	76.7 ±2.4	82.3	77.4 ±2.4	80.2	76.1 ±2.9	84.6	77.7 ±6.4	86.9	77.4 ±6.6	86.9	76.6 ±6.3	81.2	78.0 ±5.2
	XGBoost	82.0	72.5 ±0.4	81.9	76.6 ±2.4	82.2	77.2 ±2.3	80.5	76.9 ±3.0	84.6	77.4 ±6.7	86.7	77.2 ±6.7	87.3	76.3 ±5.8	81.2	77.9 ±5.1
DRO Methods	χ^2 -DRO	81.8	77.0 ±2.3	81.2	76.7 ±2.4	81.6	76.0 ±2.7	80.2	76.3 ±3.0	82.9	75.9 ±6.9	85.4	75.6 ±7.2	83.4	74.7 ±6.2	78.4	75.5 ±4.6
	CVaR-DRO	81.4	77.7 ±1.9	81.2	76.3 ±2.4	82.0	76.7 ±2.4	79.7	75.5 ±3.5	82.6	75.3 ±7.0	85.2	75.8 ±6.9	83.3	73.4 ±6.5	77.8	75.2 ±6.4
	χ^2 -DORO	81.1	77.8 ±1.7	80.4	75.1 ±2.9	81.2	75.7 ±2.7	78.8	75.9 ±2.6	78.8	70.0 ±8.2	82.1	69.9 ±8.1	82.2	70.0 ±8.1	72.4	70.2 ±6.9
	CVaR-DORO	80.9	76.7 ±2.0	80.5	75.6 ±2.7	81.1	75.2 ±2.8	79.6	75.8 ±2.7	80.7	73.0 ±7.2	84.3	75.4 ±6.7	81.9	69.9 ±8.1	76.4	74.2 ±5.8
	Group DRO	81.9	77.7 ±2.0	81.3	77.0 ±2.2	81.7	76.8 ±2.4	79.8	75.7 ±3.6	83.3	76.1 ±6.7	85.4	76.6 ±6.6	83.5	72.8 ±6.5	72.2	70.2 ±8.2
Imbalanced Learning Methods	SUBY	81.0	75.1 ±3.1	81.5	76.0 ±2.8	82.0	76.1 ±2.8	74.8	75.7 ±1.3	79.8	72.8 ±6.4	82.3	71.5 ±7.7	77.8	71.5 ±3.4	77.8	74.9 ±3.0
	RWY	81.5	75.7 ±3.0	81.8	75.9 ±2.8	82.1	76.5 ±2.7	77.7	76.2 ±1.1	80.7	75.2 ±6.4	82.5	72.2 ±7.5	83.7	74.3 ±4.5	78.7	75.6 ±3.3
	SUBG	81.9	77.3 ±2.2	81.6	76.8 ±2.4	82.0	76.9 ±2.5	80.2	76.0 ±3.2	84.3	77.4 ±6.5	86.7	77.1 ±6.7	86.3	76.1 ±5.8	80.8	77.8 ±5.2
	RWG	82.0	77.4 ±2.2	81.9	76.7 ±2.4	82.2	77.2 ±2.3	80.2	76.8 ±3.0	84.5	77.5 ±6.4	86.8	77.4 ±6.8	86.7	76.4 ±5.9	81.0	78.0 ±5.4
	JTT	78.3	74.1 ±2.5	78.1	75.3 ±1.7	79.1	75.8 ±1.8	77.9	74.7 ±2.6	80.6	74.9 ±5.1	83.1	75.6 ±5.7	84.7	75.4 ±5.7	77.6	74.2 ±4.6
	DWR	81.9	77.5 ±2.1	81.6	76.8 ±2.2	82.1	77.0 ±2.5	80.1	76.3 ±2.0	84.3	77.5 ±6.4	86.8	77.3 ±6.7	85.9	76.4 ±6.4	80.6	78.0 ±5.2
Fairness Methods	DP	81.3	76.3 ±2.4	81.0	75.4 ±2.6	81.8	76.7 ±2.4	79.3	75.5 ±3.3	84.3	77.4 ±6.4	86.6	77.2 ±6.7	86.4	76.3 ±5.8	80.6	77.8 ±5.2
	EO	81.8	77.1 ±2.3	81.8	76.5 ±2.4	82.1	77.2 ±2.4	80.0	76.7 ±2.9	84.4	77.2 ±6.7	86.8	77.1 ±6.9	86.4	76.6 ±6.3	80.8	77.7 ±4.9
	EP	81.8	77.2 ±2.3	81.9	76.5 ±2.5	82.1	77.5 ±2.2	80.3	76.2 ±3.3	84.4	77.3 ±6.6	86.8	77.3 ±6.6	86.4	76.5 ±6.2	80.9	77.6 ±4.9
	Exp	81.4	76.8 ±2.2	0.81	75.3 ±2.6	81.8	76.5 ±2.4	79.1	75.5 ±3.1	84.5	77.5 ±6.6	86.8	77.1 ±6.8	86.4	76.6 ±6.3	80.9	78.2 ±5.2
	Threshold	77.9	75.0 ±1.3	77.0	74.1 ±1.8	77.5	74.4 ±1.3	78.0	71.7 ±4.0	84.3	77.2 ±6.3	86.2	76.7 ±6.9	85.8	76.0 ±6.5	80.0	77.0 ±5.3

C.7 Worst-Domain Accuracy

Another widely-used metric in evaluating generalization performance is worst-case accuracy. In settings built on ACS Income, ACS Pub.Cov, ACS Mobility, and US Accident, for the target accuracy of each algorithm, we report the worst target domain accuracy in Table 9 and Table 10. For other settings, we do not report the worst-case accuracy because there are not many target domains, and the average& standard deviation results could reflect the population generalization performance well. In terms of the worst target accuracy for each setting, we usually observe a large performance degradation (usually over a 10 percent performance drop) in all of the existing methods. And algorithms do not show a consistent and stable ranking performance in the *o.o.d.* performance. DRO / Imbalanced learning methods can perform quite well in one *o.o.d.* setup but are dominated by other methods in some other cases. This demonstrates a need to carefully understand the difference between different domains first and develop corresponding methods then.

C.8 Average Macro-F1 Score

In consideration of the label imbalance in real-world tabular datasets, we also calculate the Macro-F1 Score for all algorithms under our settings. In this section, we report the average results in Table 11, Table 12, and Table 13. Here the standard deviation reflects the stability of out-of-distribution generalization performances (not the randomness).

Table 7. Average target domain accuracy of all algorithms on the ACS Mobility and US Accident datasets. In ACS Mobility, we test all algorithms on the 50 American states and report the mean and standard deviation across all 50 target states. And in US Accident, we choose 13 American states with relatively high sample sizes in testing. The standard deviation here reflects the stability of performances across different target states.

Dataset		ACS MOBILITY								US ACCIDENT							
Source State		NY		CA		MS		PA		CA		FL		TX		MN	
		<i>i.d.</i>	<i>o.o.d.</i>	<i>i.d.</i>	<i>o.o.d.</i>	<i>i.d.</i>	<i>o.o.d.</i>	<i>i.d.</i>	<i>o.o.d.</i>	<i>i.d.</i>	<i>o.o.d.</i>	<i>i.d.</i>	<i>o.o.d.</i>	<i>i.d.</i>	<i>o.o.d.</i>	<i>i.d.</i>	<i>o.o.d.</i>
Base	LR	78.6	72.7 ±3.6	77.1	72.7 ±3.7	77.3	72.7 ±3.7	75.4	72.7 ±3.4	83.2	70.1 ±15.4	90.7	71.7 ±13.9	95.1	74.5 ±9.6	86.4	72.2 ±11.8
	SVM	79.8	72.7 ±3.6	77.7	72.9 ±3.1	79.4	72.9 ±3.6	77.1	72.7 ±3.6	83.2	69.4 ±12.6	88.7	71.9 ±9.6	93.7	70.7 ±9.1	88.6	69.7 ±8.3
	MLP	78.7	72.7 ±3.6	77.1	72.7 ±3.7	78.1	72.4 ±3.3	75.9	73.0 ±3.1	84.7	75.7 ±10.7	92.7	78.2 ±8.7	94.9	73.0 ±9.9	88.9	74.0 ±10.2
Tree	Random Forest	80.4	74.0 ±3.1	79.0	74.1 ±3.1	80.6	73.5 ±3.4	78.6	74.3 ±3.0	86.6	77.9 ±7.8	93.5	84.4 ±10.1	95.2	84.4 ±9.9	91.6	82.0 ±5.7
	LightGBM	80.6	74.6 ±2.8	78.7	74.1 ±2.8	80.0	72.9 ±2.9	78.6	74.7 ±2.5	87.1	79.1 ±7.8	93.3	84.3 ±9.8	95.4	84.3 ±10.0	92.2	80.9 ±5.4
	XGBoost	80.4	74.6 ±3.0	0.79	74.5 ±2.8	80.9	73.5 ±3.0	79.0	74.3 ±2.4	87.1	79.8 ±7.6	94.6	82.6 ±9.3	95.3	84.4 ±9.9	92.5	79.6 ±5.4
DRO	Methods																
	χ^2 -DRO	78.5	72.7 ±3.6	77.5	72.9 ±3.4	76.8	72.7 ±3.5	76.0	73.1 ±3.3	84.4	77.3 ±9.3	92.6	73.4 ±12.6	95.0	74.6 ±9.1	89.0	72.3 ±10.4
	CVaR-DRO	78.6	72.6 ±3.5	77.2	72.8 ±3.5	77.7	72.6 ±3.7	75.7	73.3 ±3.2	84.7	74.5 ±10.3	92.7	74.4 ±11.4	95.0	74.9 ±9.4	89.5	73.4 ±10.0
	χ^2 -DORO	78.6	72.6 ±3.6	77.8	72.8 ±3.3	77.1	72.7 ±3.7	75.3	72.7 ±3.7	84.7	72.9 ±11.5	92.3	77.6 ±8.9	94.3	74.3 ±9.6	87.6	74.7 ±8.7
	CVaR-DORO	78.7	72.7 ±3.6	78.0	73.6 ±3.1	77.4	72.7 ±3.7	75.3	72.7 ±3.6	84.9	74.1 ±10.5	92.8	74.4 ±11.2	94.9	74.7 ±9.5	89.1	74.1 ±9.5
Group DRO	78.6	72.5 ±3.4	77.1	72.7 ±3.6	76.0	72.7 ±3.7	76.0	72.8 ±3.2	N/A	N/A	N/A	N/A	N/A	N/A	N/A	N/A	
Imbalanced Learning	Methods																
	SUBY	78.2	72.7 ±3.5	76.3	72.5 ±3.6	76.6	70.0 ±2.8	74.7	69.5 ±2.0	86.5	85.4 ±7.3	93.7	84.6 ±10.0	95.2	84.4 ±9.9	91.8	83.8 ±6.6
	RWY	78.5	72.7 ±3.6	76.7	72.7 ±3.6	76.5	72.2 ±3.4	74.5	72.6 ±3.7	86.9	82.2 ±7.1	93.4	84.5 ±10.2	95.3	84.3 ±10.0	92.5	81.1 ±5.4
	SUBG	80.2	74.3 ±2.9	79.2	74.2 ±2.8	79.5	72.5 ±2.9	78.6	74.3 ±2.7	86.3	81.0 ±7.3	93.0	83.8 ±9.9	95.1	84.4 ±9.9	91.1	80.1 ±5.8
	RWG	80.3	74.6 ±3.0	79.1	74.4 ±2.8	80.1	73.3 ±2.9	78.7	74.2 ±2.6	87.5	79.7 ±7.5	93.4	83.8 ±9.4	95.2	84.4 ±9.9	92.4	79.3 ±5.3
	JTT	78.3	72.7 ±3.6	76.5	72.4 ±3.7	77.6	71.5 ±2.6	75.1	70.7 ±2.4	86.5	79.0 ±7.7	92.7	83.6 ±9.5	94.9	84.3 ±9.9	91.8	78.2 ±5.6
DWR	79.7	74.2 ±3.1	78.3	73.9 ±2.9	79.1	72.9 ±2.9	77.5	74.0 ±2.6	87.2	79.8 ±7.7	93.4	83.7 ±9.9	95.3	84.4 ±9.9	92.3	78.5 ±5.8	
Fairness	Methods																
	DP	80.5	74.7 ±2.8	78.8	74.2 ±2.9	80.0	73.8 ±3.1	78.3	74.0 ±2.6	86.6	79.7 ±7.5	92.8	83.9 ±9.5	94.8	84.3 ±9.9	91.9	81.9 ±5.8
	EO	80.3	74.7 ±2.8	78.9	74.1 ±2.8	79.8	73.4 ±3.0	78.5	73.9 ±2.7	86.6	79.5 ±7.5	93.2	84.4 ±9.6	95.2	84.4 ±10.1	92.2	79.6 ±5.4
	EP	80.3	74.7 ±2.8	78.9	74.1 ±3.0	80.1	74.0 ±3.0	78.4	74.1 ±2.7	87.0	80.3 ±7.5	93.3	84.2 ±9.9	95.1	84.4 ±10.0	91.9	79.6 ±5.2
	Exp	80.5	74.8 ±2.9	78.9	74.1 ±2.9	81.0	73.9 ±2.9	78.4	74.3 ±2.6	85.9	78.6 ±7.3	90.1	82.3 ±9.1	93.1	81.6 ±9.6	86.3	80.4 ±6.0
Threshold	80.5	74.5 ±2.9	78.6	74.3 ±2.8	78.2	71.9 ±2.9	78.5	73.9 ±2.6	84.3	77.8 ±7.3	88.1	79.9 ±7.9	91.2	79.9 ±9.3	82.0	75.7 ±4.8	

Table 8. Average target domain accuracy of all algorithms on the Taxi, ACS Pub.Cov (Temporal) and ACS Income (Synthetic) datasets. In Taxi and ACS Pub.Cov (Temporal), we test all algorithms on the 3 target domains and report the mean and standard deviation across all 3 target domains. The standard deviation here reflects the stability of performances across different target states. In ACS Income (Synthetic), we simulate strong covariate shifts according to the "Age" feature, where 10% and 20% means the minor group ratio in training, respectively.

Dataset		Taxi				ACS Pub.Cov (Temporal)				ACS Income (Synthetic)			
		BOG		NYC		NY		CA		20%		10%	
Source		<i>i.d.</i>	<i>o.o.d</i>	<i>i.d.</i>	<i>o.o.d</i>	<i>i.d.</i>	<i>o.o.d</i>	<i>i.d.</i>	<i>o.o.d</i>	<i>i.d.</i>	<i>o.o.d</i>	<i>i.d.</i>	<i>o.o.d</i>
Base Methods	LR	75.6	71.2 \pm 2.0	83.6	74.2 \pm 1.2	76.3	68.5 \pm 2.3	80.8	68.2 \pm 4.0	92.2	81.6	94.0	79.3
	SVM	75.7	76.1 \pm 3.1	83.4	74.4 \pm 1.4	77.4	69.1 \pm 2.0	80.7	67.7 \pm 3.9	92.0	80.0	94.1	79.5
	MLP	77.7	70.0 \pm 1.3	84.5	73.7 \pm 0.6	78.0	70.6 \pm 2.4	82.5	70.3 \pm 3.8	92.5	82.1	94.3	79.5
Tree Ensemble Methods	Random Forest	76.1	77.5 \pm 4.7	85.7	71.6 \pm 0.9	79.1	71.3 \pm 2.5	83.4	70.4 \pm 4.1	92.7	81.7	94.4	78.5
	LightGBM	86.3	73.2 \pm 4.3	87.0	72.0 \pm 0.9	79.7	72.1 \pm 2.4	84.0	70.7 \pm 3.9	92.6	83.0	94.2	80.4
	XGBoost	85.0	71.5 \pm 2.7	86.7	72.5 \pm 1.0	79.3	71.9 \pm 2.6	83.6	71.1 \pm 3.7	92.7	82.2	94.4	79.7
DRO Methods	χ^2 -DRO	77.4	72.2 \pm 2.4	84.6	73.0 \pm 0.8	77.3	69.0 \pm 2.5	81.9	70.0 \pm 3.8	92.5	81.3	94.2	79.7
	CVaR-DRO	77.0	73.4 \pm 2.5	85.9	72.8 \pm 0.6	76.6	69.1 \pm 2.4	82.2	69.1 \pm 4.5	92.5	81.2	94.3	79.0
	χ^2 -DORO	75.8	73.3 \pm 2.9	84.9	73.9 \pm 0.8	71.7	61.2 \pm 3.5	79.7	64.8 \pm 3.9	92.3	81.4	93.8	77.4
	CVaR-DORO	75.6	74.3 \pm 3.0	85.1	73.8 \pm 0.8	76.0	67.9 \pm 2.6	79.5	64.9 \pm 4.0	92.5	81.4	93.9	76.7
	Group DRO	N/A	N/A	N/A	N/A	76.8	70.5 \pm 2.1	81.9	70.0 \pm 3.9	92.5	81.4	94.2	79.8
Imbalanced Learning Methods	SUBY	87.2	67.1 \pm 1.6	85.9	70.8 \pm 0.5	73.9	69.8 \pm 1.3	81.4	68.3 \pm 3.8	87.0	69.9	88.5	64.2
	RWY	81.2	73.0 \pm 1.4	86.7	72.4 \pm 0.7	75.1	70.9 \pm 1.6	79.4	65.8 \pm 4.1	90.3	78.6	92.1	76.3
	SUBG	86.3	72.5 \pm 4.4	85.6	71.4 \pm 0.9	79.4	71.8 \pm 2.3	83.7	70.7 \pm 3.6	92.6	81.7	94.4	79.5
	RWG	81.1	69.1 \pm 3.6	86.5	71.3 \pm 0.9	79.4	72.8 \pm 2.2	83.8	70.8 \pm 3.7	92.6	82.7	94.5	80.1
	JTT	84.6	69.5 \pm 0.9	85.4	71.2 \pm 0.8	73.8	66.7 \pm 2.3	79.5	67.4 \pm 3.5	91.5	78.9	93.5	76.5
DWR	82.9	68.2 \pm 1.9	83.7	70.7 \pm 0.9	79.2	71.3 \pm 2.4	83.8	70.7 \pm 3.9	92.5	82.6	94.2	80.3	
Fairness Methods	DP	84.1	70.2 \pm 4.0	86.3	72.0 \pm 0.8	79.6	72.7 \pm 2.0	83.7	71.1 \pm 3.9	92.5	82.7	94.2	80.2
	EO	81.1	71.9 \pm 3.0	87.1	71.8 \pm 0.8	79.5	72.3 \pm 2.5	83.4	70.1 \pm 4.0	92.6	81.7	94.3	79.5
	EP	79.7	71.6 \pm 1.7	85.7	70.9 \pm 0.6	79.6	72.5 \pm 2.1	83.6	71.0 \pm 3.9	92.4	82.6	94.2	80.0
	Exp	79.2	68.6 \pm 0.4	84.9	71.6 \pm 0.6	79.3	72.3 \pm 2.3	83.4	71.1 \pm 4.2	92.6	81.9	94.3	79.4
	Threshold	80.8	69.8 \pm 1.7	84.3	59.7 \pm 3.9	79.2	71.9 \pm 2.2	83.4	70.4 \pm 3.9	91.8	78.3	93.5	74.0

Table 9. Worst target domain accuracy of all algorithms on the ACS Income and ACS Pub.Cov datasets. In each setting, we test all algorithms on the 50 American states and report the worst accuracy among all 50 target states.

Dataset		ACS INCOME								ACS PUB.COVS							
Source State		CA		CT		MA		SD		FL		TX		NE		IN	
		<i>i.d.</i>	<i>o.o.d.</i>	<i>i.d.</i>	<i>o.o.d.</i>	<i>i.d.</i>	<i>o.o.d.</i>	<i>i.d.</i>	<i>o.o.d.</i>	<i>i.d.</i>	<i>o.o.d.</i>	<i>i.d.</i>	<i>o.o.d.</i>	<i>i.d.</i>	<i>o.o.d.</i>	<i>i.d.</i>	<i>o.o.d.</i>
Base Methods	LR	81.1	72.3	80.7	70.5	80.9	71.1	80.1	69.4	81.3	49.6	84.1	49.0	84.3	0.52	78.6	54.7
	SVM	79.4	67.1	78.6	61.6	80.1	62.2	79.3	64.6	80.5	53.0	84.2	50.3	84.8	50.4	77.1	57.4
	MLP	81.8	68.3	81.4	70.8	81.7	71.3	80.5	70.5	83.3	54.3	85.4	53.9	84.5	52.9	78.8	56.7
Tree Ensemble Methods	Random Forest	81.7	72.6	81.2	71.6	81.5	71.2	80.2	68.3	84.6	54.2	86.8	52.8	86.7	52.9	81.2	59.0
	LightGBM	81.8	71.1	82.1	69.5	82.3	70.1	80.2	69.6	84.6	56.9	86.9	53.9	86.9	52.3	81.2	60.4
	XGBoost	82.0	72.2	81.9	70.1	82.2	70.9	80.5	70.5	84.6	54.8	86.7	53.7	87.3	55.4	81.2	59.6
DRO Methods	χ^2 -DRO	81.8	69.7	81.2	69.7	81.6	67.9	80.2	70.3	82.9	52.5	85.4	50.5	83.4	52.9	78.4	62.4
	CVaR-DRO	81.4	72.1	81.2	70.7	82.0	70.0	79.7	68.4	82.6	52.2	85.2	51.7	83.3	52.3	77.8	53.9
	χ^2 -DORO	81.1	70.3	80.4	62.6	81.2	63.8	78.8	69.5	78.8	43.6	82.1	43.6	82.2	43.6	72.4	49.9
	CVaR-DORO	80.9	68.7	80.5	64.9	81.1	64.3	79.6	69.1	80.7	49.5	84.3	52.4	81.9	43.6	76.4	56.2
	Group DRO	81.9	72.6	81.3	71.8	81.7	69.2	79.8	0.68	83.3	53.2	85.4	53.2	83.5	51.3	72.2	43.6
Imbalanced Learning Methods	SUBY	81.0	65.2	81.5	68.0	82.0	66.3	74.8	72.5	79.8	51.3	82.3	45.4	77.8	64.5	77.8	68.3
	RWY	81.5	65.2	81.8	68.3	82.1	67.6	77.7	73.2	80.7	53.3	82.5	45.6	83.7	57.1	78.7	65.8
	SUBG	81.9	71.4	81.6	70.1	82.0	68.4	80.2	70.3	84.3	56.1	86.7	53.0	86.3	53.6	80.8	60.2
	RWG	82.0	71.3	81.9	70.6	82.2	70.3	80.2	70.6	84.5	56.8	86.8	52.1	86.7	55.1	81.0	57.2
	JTT	78.3	68.4	78.1	71.2	79.1	71.6	77.9	68.6	80.6	59.4	83.1	56.2	84.7	55.4	77.6	56.7
	DWR	81.9	71.2	81.6	71.0	82.1	69.0	80.1	72.0	84.3	58.1	86.8	54.2	85.9	52.8	80.6	59.4
Fairness Methods	DP	81.3	70.3	81.0	68.8	81.8	70.7	79.3	68.4	84.3	57.4	86.6	53.7	86.4	52.9	80.6	57.8
	EO	81.8	70.6	81.8	70.5	82.1	70.8	80.0	70.6	84.4	55.4	86.8	53.6	86.4	53.6	80.8	61.6
	EP	81.8	70.7	81.9	69.8	82.1	70.9	80.3	69.2	84.4	55.5	86.8	54.4	86.4	53.6	80.9	60.1
	Exp	81.4	70.6	81.0	69.4	81.8	70.4	79.1	68.8	84.5	55.4	86.8	52.8	86.4	52.5	80.9	61.5
	Threshold	77.9	71.8	77.0	69.8	77.5	70.9	78.0	62.8	84.3	57.3	86.2	52.4	85.8	52.9	80.0	59.9

Table 10. Worst target domain accuracy of all algorithms on the ACS Mobility and US Accident datasets. In ACS Mobility, we test all algorithms on the 50 American states and report the worst accuracy among all 50 target states. And in US Accident, we choose 13 American states with relatively high sample sizes in testing.

Dataset		ACS MOBILITY								US ACCIDENT							
Source State		NY		CA		MS		PA		CA		FL		TX		MN	
		<i>i.d.</i>	<i>o.o.d.</i>	<i>i.d.</i>	<i>o.o.d.</i>	<i>i.d.</i>	<i>o.o.d.</i>	<i>i.d.</i>	<i>o.o.d.</i>	<i>i.d.</i>	<i>o.o.d.</i>	<i>i.d.</i>	<i>o.o.d.</i>	<i>i.d.</i>	<i>o.o.d.</i>	<i>i.d.</i>	<i>o.o.d.</i>
Base Methods	LR	78.6	64.7	77.1	64.6	77.3	64.8	75.4	66.3	83.2	44.9	90.7	48.3	95.1	57.4	86.4	52.8
	SVM	79.8	64.6	77.7	66.8	79.4	65.3	77.1	64.7	83.2	49.2	88.7	58.3	93.7	55.7	88.6	56.1
	MLP	78.7	64.7	77.1	64.8	78.1	66.3	75.9	67.0	84.7	58.4	92.7	61.1	94.9	57.2	88.9	57.1
Tree Ensemble Methods	Random Forest	80.4	68.0	79.0	68.2	80.6	67.5	78.6	68.7	86.6	66.6	93.5	58.2	95.2	58.5	91.6	68.0
	LightGBM	80.6	68.7	78.7	69.0	80.0	67.9	78.6	69.8	87.1	65.3	93.3	59.0	95.4	58.6	92.2	68.1
	XGBoost	80.4	68.6	79.0	69.0	80.9	68.3	79.0	69.4	87.1	65.6	94.6	59.0	95.3	58.8	92.5	68.5
DRO Methods	χ^2 -DRO	78.5	65.1	77.5	66.6	76.8	65.4	76.0	67.1	84.4	62.9	92.6	53.3	95.0	57.9	89.0	53.5
	CVaR-DRO	78.6	65.0	77.2	65.6	77.7	64.4	75.7	67.6	84.7	57.2	92.7	57.5	95.0	58.4	89.5	56.3
	χ^2 -DORO	78.6	64.3	77.8	66.9	77.1	64.7	75.3	64.7	84.7	53.9	92.3	61.1	94.3	57.0	87.6	59.8
	CVaR-DORO	78.7	64.7	78.0	67.4	77.4	64.7	75.3	64.9	84.9	57.8	92.8	58.1	94.9	57.5	89.1	57.6
	Group DRO	78.6	65.5	77.1	65.1	76.0	64.5	76.0	66.8	N/A	N/A	N/A	N/A	N/A	N/A	N/A	N/A
Imbalanced Learning Methods	SUBY	78.2	65.0	76.3	64.6	76.6	64.7	74.7	65.0	86.5	64.2	93.7	58.8	95.2	58.5	91.8	65.6
	RWY	78.5	64.7	76.7	65.0	76.5	65.6	74.5	64.6	86.9	64.8	93.4	58.3	95.3	58.5	92.5	67.5
	SUBG	80.2	68.8	79.2	68.9	79.5	67.0	78.6	69.2	86.3	66.4	93.0	58.1	95.1	58.4	91.1	67.4
	RWG	80.3	68.4	79.1	69.4	80.1	68.3	78.7	69.4	87.5	65.4	93.4	59.4	95.2	58.4	92.4	68.6
	JTT	78.3	64.7	76.5	64.7	77.6	66.6	75.1	65.6	86.5	65.9	92.7	58.6	94.9	58.6	91.8	68.2
	DWR	79.7	67.4	78.3	68.5	79.1	67.4	77.5	69.0	87.2	65.8	93.4	58.1	95.3	58.5	92.3	67.6
Fairness Methods	DP	80.5	69.2	78.8	68.4	80.0	68.2	78.3	68.7	86.6	65.2	92.8	59.0	94.8	58.4	91.9	66.6
	EO	80.3	69.3	78.9	68.9	79.8	0.68	78.5	68.5	86.6	65.6	93.2	58.8	95.2	58.5	92.2	68.1
	EP	80.3	68.7	78.9	68.5	80.1	68.1	78.4	68.5	87.0	65.6	93.3	59.0	95.1	58.6	91.9	67.9
	Exp	80.5	69.0	78.9	68.6	81.0	68.8	78.4	69.0	85.9	65.4	90.1	58.7	93.1	56.5	86.3	64.7
	Threshold	80.5	69.0	78.6	69.2	78.2	66.7	78.5	68.7	84.3	64.5	88.1	59.5	91.2	55.7	82.0	64.0

Table 11. Average target domain Macro-F1 score of all algorithms on the ACS Income and ACS Pub.Cov datasets. In each setting, we test all algorithms on the 50 American states and report the mean and standard deviation across all 50 target states. The standard deviation here reflects the stability of performances across different target states.

Dataset		ACS Income								ACS Pub.Cov							
Source State		CA		CT		MA		IN		FL		TX		NE		IN	
		<i>i.d.</i>	<i>o.o.d.</i>														
Base Methods	LR	0.804	0.757 ±0.032	0.807	0.747 ±0.035	0.809	0.752 ±0.034	0.714	0.692 ±0.019	0.652	0.620 ±0.050	0.644	0.580 ±0.052	0.653	0.612 ±0.046	0.698	0.659 ±0.044
	SVM	0.795	0.726 ±0.037	0.790	0.709 ±0.039	0.793	0.718 ±0.041	0.698	0.664 ±0.023	0.663	0.623 ±0.044	0.665	0.614 ±0.044	0.698	0.611 ±0.043	0.696	0.650 ±0.032
	MLP	0.814	0.751 ±0.038	0.814	0.753 ±0.036	0.816	0.755 ±0.037	0.734	0.729 ±0.018	0.709	0.664 ±0.049	0.713	0.664 ±0.049	0.698	0.644 ±0.046	0.716	0.680 ±0.038
Tree Ensemble Methods	Random Forest	0.809	0.759 ±0.032	0.812	0.755 ±0.034	0.814	0.758 ±0.034	0.687	0.673 ±0.024	0.715	0.659 ±0.055	0.727	0.651 ±0.058	0.729	0.648 ±0.046	0.746	0.691 ±0.039
	LightGBM	0.811	0.757 ±0.035	0.821	0.753 ±0.037	0.823	0.759 ±0.037	0.732	0.718 ±0.021	0.730	0.670 ±0.053	0.739	0.665 ±0.057	0.745	0.663 ±0.048	0.750	0.704 ±0.034
	XGBoost	0.814	0.651 ±0.049	0.819	0.751 ±0.036	0.822	0.757 ±0.036	0.723	0.708 ±0.021	0.723	0.673 ±0.051	0.730	0.659 ±0.058	0.755	0.667 ±0.042	0.747	0.701 ±0.038
DRO Methods	χ ² -DRO	0.813	0.754 ±0.036	0.812	0.752 ±0.036	0.816	0.748 ±0.039	0.732	0.737 ±0.019	0.704	0.659 ±0.044	0.697	0.657 ±0.048	0.685	0.646 ±0.038	0.715	0.673 ±0.030
	CVaR-DRO	0.808	0.750 ±0.038	0.812	0.749 ±0.036	0.820	0.752 ±0.037	0.730	0.726 ±0.021	0.693	0.649 ±0.046	0.706	0.655 ±0.049	0.668	0.658 ±0.021	0.700	0.675 ±0.036
	χ ² -DORO	0.801	0.756 ±0.032	0.804	0.738 ±0.041	0.812	0.744 ±0.040	0.717	0.711 ±0.018	0.526	0.511 ±0.013	0.518	0.481 ±0.021	0.526	0.491 ±0.016	0.516	0.487 ±0.021
	CVaR-DORO	0.802	0.746 ±0.037	0.804	0.740 ±0.041	0.811	0.740 ±0.041	0.720	0.706 ±0.020	0.660	0.619 ±0.044	0.675	0.629 ±0.052	0.559	0.541 ±0.025	0.649	0.623 ±0.023
	Group DRO	0.812	0.760 ±0.033	0.813	0.754 ±0.035	0.817	0.753 ±0.037	0.741	0.742 ±0.018	0.706	0.665 ±0.051	0.717	0.660 ±0.050	0.700	0.635 ±0.042	0.419	0.411 ±0.030
Imbalanced Learning Methods	SUBY	0.807	0.739 ±0.041	0.815	0.748 ±0.039	0.820	0.750 ±0.040	0.719	0.739 ±0.025	0.710	0.699 ±0.023	0.710	0.692 ±0.027	0.704	0.682 ±0.031	0.748	0.710 ±0.025
	RWY	0.812	0.747 ±0.041	0.818	0.747 ±0.039	0.821	0.753 ±0.039	0.733	0.732 ±0.020	0.725	0.705 ±0.025	0.729	0.699 ±0.032	0.736	0.680 ±0.031	0.749	0.709 ±0.024
	SUBG	0.813	0.759 ±0.034	0.816	0.753 ±0.036	0.820	0.758 ±0.037	0.726	0.715 ±0.021	0.719	0.671 ±0.048	0.731	0.662 ±0.053	0.739	0.666 ±0.041	0.742	0.686 ±0.034
	RWG	0.814	0.760 ±0.035	0.819	0.754 ±0.036	0.822	0.757 ±0.036	0.726	0.723 ±0.019	0.723	0.667 ±0.051	0.733	0.661 ±0.057	0.748	0.672 ±0.045	0.746	0.700 ±0.035
	JTT	0.777	0.728 ±0.036	0.781	0.733 ±0.030	0.79	0.739 ±0.031	0.710	0.702 ±0.017	0.711	0.690 ±0.027	0.726	0.691 ±0.038	0.727	0.669 ±0.036	0.718	0.669 ±0.031
DWR	0.812	0.759 ±0.035	0.816	0.755 ±0.034	0.821	0.756 ±0.037	0.733	0.719 ±0.019	0.721	0.668 ±0.047	0.731	0.661 ±0.057	0.732	0.676 ±0.041	0.741	0.697 ±0.033	
Fairness Methods	DP	0.807	0.746 ±0.037	0.810	0.740 ±0.038	0.817	0.752 ±0.037	0.716	0.708 ±0.017	0.727	0.677 ±0.049	0.729	0.659 ±0.054	0.750	0.668 ±0.043	0.742	0.698 ±0.032
	EO	0.813	0.757 ±0.035	0.818	0.752 ±0.036	0.820	0.757 ±0.037	0.721	0.709 ±0.020	0.724	0.668 ±0.054	0.734	0.661 ±0.052	0.737	0.671 ±0.044	0.748	0.704 ±0.031
	EP	0.811	0.759 ±0.035	0.819	0.752 ±0.037	0.821	0.756 ±0.037	0.723	0.709 ±0.018	0.724	0.668 ±0.051	0.731	0.657 ±0.058	0.747	0.671 ±0.039	0.748	0.699 ±0.034
	Exp	0.808	0.750 ±0.037	0.810	0.737 ±0.038	0.818	0.749 ±0.037	0.706	0.691 ±0.021	0.724	0.667 ±0.053	0.729	0.656 ±0.057	0.738	0.661 ±0.049	0.741	0.699 ±0.033
	Threshold	0.766	0.709 ±0.037	0.768	0.718 ±0.032	0.771	0.716 ±0.028	0.665	0.669 ±0.019	0.722	0.669 ±0.050	0.717	0.652 ±0.056	0.714	0.644 ±0.040	0.728	0.681 ±0.031

Table 12. Average target domain Macro-F1 score of all algorithms on the ACS Mobility and US Accident datasets. In ACS Mobility, we test all algorithms on the 50 American states and report the mean and standard deviation across all 50 target states. And in US Accident, we choose 13 American states with relatively high sample sizes in testing. The standard deviation here reflects the stability of performances across different target states.

Dataset		ACS Mobility								US Accident							
Source State		NY		CA		MS		PA		CA		FL		TX		MN	
		<i>i.d.</i>	<i>o.o.d.</i>														
Base Methods	LR	0.451	0.427 ±0.015	0.462	0.446 ±0.026	0.531	0.488 ±0.020	0.527	0.488 ±0.020	0.800	0.678 ±0.147	0.898	0.703 ±0.133	0.936	0.736 ±0.092	0.855	0.703 ±0.110
	SVM	0.604	0.572 ±0.015	0.592	0.550 ±0.014	0.635	0.532 ±0.018	0.623	0.581 ±0.018	0.793	0.674 ±0.114	0.891	0.698 ±0.093	0.928	0.698 ±0.093	0.880	0.669 ±0.078
	MLP	0.600	0.583 ±0.020	0.622	0.607 ±0.018	0.607	0.583 ±0.012	0.608	0.578 ±0.020	0.827	0.755 ±0.103	0.923	0.769 ±0.090	0.934	0.720 ±0.094	0.886	0.713 ±0.096
Tree Ensemble Methods	Random Forest	0.570	0.530 ±0.019	0.587	0.563 ±0.023	0.641	0.534 ±0.022	0.635	0.561 ±0.025	0.846	0.752 ±0.077	0.932	0.832 ±0.096	0.938	0.834 ±0.095	0.911	0.800 ±0.058
	LightGBM	0.637	0.589 ±0.014	0.625	0.601 ±0.019	0.671	0.590 ±0.021	0.660	0.590 ±0.015	0.851	0.768 ±0.075	0.929	0.831 ±0.094	0.940	0.833 ±0.096	0.918	0.786 ±0.054
	XGBoost	0.637	0.591 ±0.018	0.625	0.605 ±0.018	0.678	0.586 ±0.023	0.664	0.596 ±0.017	0.852	0.786 ±0.072	0.942	0.812 ±0.088	0.939	0.833 ±0.095	0.920	0.771 ±0.052
DRO Methods	χ ² -DRO	0.613	0.613 ±0.019	0.599	0.579 ±0.015	0.540	0.514 ±0.031	0.606	0.583 ±0.017	0.824	0.754 ±0.099	0.922	0.721 ±0.121	0.933	0.747 ±0.091	0.883	0.704 ±0.095
	CVaR-DRO	0.621	0.612 ±0.017	0.628	0.603 ±0.015	0.574	0.565 ±0.025	0.639	0.613 ±0.021	0.825	0.742 ±0.094	0.924	0.731 ±0.111	0.936	0.740 ±0.090	0.888	0.716 ±0.092
	χ ² -DORO	0.509	0.501 ±0.011	0.619	0.612 ±0.018	0.530	0.505 ±0.013	0.540	0.508 ±0.014	0.815	0.707 ±0.104	0.920	0.760 ±0.089	0.927	0.734 ±0.092	0.874	0.727 ±0.080
	CVaR-DORO	0.533	0.524 ±0.011	0.625	0.578 ±0.019	0.521	0.500 ±0.008	0.510	0.477 ±0.016	0.825	0.748 ±0.090	0.922	0.732 ±0.110	0.934	0.738 ±0.092	0.887	0.729 ±0.094
	Group DRO	0.588	0.567 ±0.018	0.566	0.528 ±0.020	0.564	0.536 ±0.019	0.595	0.555 ±0.021	N/A	N/A	N/A	N/A	N/A	N/A	N/A	N/A
Imbalanced Learning Methods	SUBY	0.657	0.628 ±0.017	0.649	0.603 ±0.017	0.674	0.621 ±0.016	0.678	0.629 ±0.019	0.854	0.839 ±0.073	0.933	0.834 ±0.095	0.938	0.833 ±0.095	0.915	0.821 ±0.066
	RWY	0.657	0.627 ±0.017	0.647	0.610 ±0.014	0.678	0.621 ±0.017	0.677	0.633 ±0.018	0.856	0.845 ±0.076	0.930	0.834 ±0.097	0.940	0.833 ±0.095	0.920	0.790 ±0.055
	SUBG	0.635	0.589 ±0.016	0.624	0.601 ±0.020	0.672	0.595 ±0.020	0.658	0.592 ±0.018	0.847	0.790 ±0.073	0.925	0.826 ±0.094	0.937	0.833 ±0.095	0.906	0.784 ±0.057
	RWG	0.637	0.587 ±0.018	0.621	0.584 ±0.016	0.676	0.582 ±0.018	0.663	0.596 ±0.018	0.855	0.775 ±0.074	0.929	0.825 ±0.089	0.938	0.833 ±0.095	0.919	0.768 ±0.051
	JTT	0.639	0.594 ±0.014	0.616	0.574 ±0.013	0.660	0.589 ±0.019	0.639	0.584 ±0.017	0.843	0.786 ±0.074	0.922	0.823 ±0.091	0.935	0.833 ±0.095	0.912	0.766 ±0.052
DWR	0.622	0.581 ±0.013	0.620	0.605 ±0.020	0.656	0.585 ±0.018	0.647	0.597 ±0.018	0.853	0.777 ±0.075	0.929	0.824 ±0.094	0.939	0.833 ±0.094	0.917	0.759 ±0.054	
Fairness Methods	DP	0.630	0.588 ±0.014	0.621	0.590 ±0.014	0.663	0.590 ±0.020	0.668	0.593 ±0.018	0.847	0.776 ±0.073	0.922	0.814 ±0.085	0.933	0.832 ±0.095	0.915	0.799 ±0.059
	EO	0.632	0.590 ±0.018	0.625	0.602 ±0.019	0.665	0.593 ±0.022	0.662	0.597 ±0.020	0.846	0.771 ±0.077	0.926	0.831 ±0.091	0.938	0.833 ±0.096	0.917	0.772 ±0.051
	EP	0.633	0.596 ±0.017	0.620	0.598 ±0.017	0.671	0.581 ±0.015	0.660	0.593 ±0.017	0.852	0.787 ±0.071	0.928	0.830 ±0.094	0.937	0.832 ±0.097	0.914	0.773 ±0.049
	Exp	0.633	0.589 ±0.015	0.622	0.594 ±0.020	0.669	0.595 ±0.020	0.663	0.595 ±0.016	0.837	0.769 ±0.079	0.893	0.808 ±0.085	0.909	0.803 ±0.091	0.854	0.784 ±0.060
	Threshold	0.629	0.587 ±0.013	0.620	0.596 ±0.019	0.661	0.571 ±0.019	0.658	0.597 ±0.022	0.820	0.755 ±0.069	0.870	0.782 ±0.074	0.885	0.787 ±0.086	0.809	0.730 ±0.045

Table 13. Average target domain Macro-F1 score of all algorithms on the Taxi, ACS Pub.Cov (Temporal) and ACS Income (Synthetic) datasets. In Taxi and ACS Pub.Cov (Temporal), we test all algorithms on the 3 target domains and report the mean and standard deviation across all 3 target domains. The standard deviation here reflects the stability of performances across different target states. In ACS Income (Synthetic), we simulate strong covariate shifts according to the "Age" feature, where 10% and 20% means the minor group ratio in training, respectively.

Dataset		Taxi				ACS Pub.Cov (Temporal)				ACS Income (Synthetic)			
Source		BOG		NYC		NY		CA		20%		10%	
		<i>i.d.</i>	<i>o.o.d.</i>	<i>i.d.</i>	<i>o.o.d.</i>	<i>i.d.</i>	<i>o.o.d.</i>	<i>i.d.</i>	<i>o.o.d.</i>	<i>i.d.</i>	<i>o.o.d.</i>	<i>i.d.</i>	<i>o.o.d.</i>
Base Methods	LR	0.754	0.695 ±0.007	0.802	0.731 ±0.014	0.641	0.599 ±0.009	0.586	0.528 ±0.024	0.797	0.799	0.766	0.780
	SVM	0.757	0.761 ±0.036	0.809	0.735 ±0.019	0.663	0.613 ±0.013	0.612	0.556 ±0.016	0.795	0.764	N/A	N/A
	MLP	0.757	0.684 ±0.012	0.823	0.719 ±0.008	0.692	0.652 ±0.012	0.674	0.587 ±0.030	0.817	0.796	0.792	0.762
Tree Ensemble Methods	Random Forest	0.760	0.762 ±0.032	0.840	0.718 ±0.018	0.692	0.648 ±0.016	0.663	0.571 ±0.032	0.810	0.797	0.782	0.777
	LightGBM	0.866	0.717 ±0.029	0.841	0.701 ±0.011	0.711	0.668 ±0.016	0.683	0.595 ±0.027	0.817	0.813	0.787	0.788
	XGBoost	0.839	0.695 ±0.015	0.846	0.723 ±0.017	0.715	0.679 ±0.014	0.689	0.591 ±0.034	0.815	0.801	0.787	0.788
DRO Methods	χ ² -DRO	0.776	0.693 ±0.016	0.830	0.726 ±0.009	0.675	0.633 ±0.016	0.663	0.580 ±0.031	0.820	0.788	0.790	0.783
	CVaR-DRO	0.767	0.744 ±0.032	0.835	0.732 ±0.010	0.668	0.625 ±0.014	0.654	0.586 ±0.025	0.820	0.799	0.791	0.783
	χ ² -DORO	0.750	0.752 ±0.027	0.816	0.732 ±0.009	0.568	0.540 ±0.014	0.531	0.501 ±0.010	0.810	0.796	0.778	0.766
	CVaR-DORO	0.756	0.724 ±0.023	0.829	0.730 ±0.006	0.652	0.610 ±0.017	0.618	0.556 ±0.021	0.812	0.781	0.778	0.763
	Group DRO	N/A	N/A	N/A	N/A	0.682	0.655 ±0.010	0.667	0.605 ±0.020	0.814	0.798	0.795	0.763
Imbalanced Learning Methods	SUBY	0.859	0.669 ±0.014	0.835	0.708 ±0.014	0.706	0.690 ±0.009	0.678	0.660 ±0.010	0.774	0.699	0.716	0.562
	RWY	0.811	0.737 ±0.033	0.840	0.713 ±0.017	0.716	0.703 ±0.009	0.693	0.656 ±0.019	0.795	0.780	0.768	0.765
	SUBG	0.858	0.712 ±0.032	0.837	0.701 ±0.013	0.707	0.692 ±0.013	0.687	0.588 ±0.033	0.816	0.802	0.788	0.783
	RWG	0.802	0.731 ±0.035	0.840	0.720 ±0.018	0.713	0.654 ±0.015	0.686	0.601 ±0.034	0.816	0.810	0.798	0.791
	JTT	0.842	0.686 ±0.003	0.830	0.704 ±0.017	0.677	0.654 ±0.011	0.676	0.641 ±0.016	0.801	0.780	0.772	0.750
Fairness Methods	DWR	0.845	0.671 ±0.016	0.813	0.673 ±0.015	0.713	0.675 ±0.017	0.685	0.604 ±0.029	0.817	0.812	0.785	0.785
	DP	0.842	0.696 ±0.020	0.843	0.702 ±0.014	0.712	0.671 ±0.016	0.689	0.600 ±0.031	0.815	0.813	0.785	0.795
	EO	0.813	0.727 ±0.028	0.846	0.706 ±0.015	0.713	0.670 ±0.018	0.686	0.586 ±0.031	0.814	0.798	0.782	0.789
	EP	0.801	0.728 ±0.027	0.835	0.710 ±0.018	0.712	0.671 ±0.016	0.687	0.597 ±0.031	0.814	0.815	0.786	0.786
	Exp	0.797	0.724 ±0.034	0.838	0.702 ±0.015	0.712	0.648 ±0.018	0.685	0.597 ±0.033	0.814	0.798	0.783	0.783
	Threshold	0.806	0.660 ±0.003	0.812	0.536 ±0.027	0.711	0.670 ±0.018	0.688	0.605 ±0.030	0.785	0.786	0.752	0.761

C.9 Worst-Domain Macro-F1 Score

In settings built on ACS Income, ACS Pub.Cov, ACS Mobility, and US Accident, for the target accuracy of each algorithm, we report the worst target domain Macro-F1 score in Table 14 and Table 15. For other settings, we do not report the worst-case results because there are not many target domains there and the mean/standard deviation results could reflect the generalization performance well.

For the results of Macro-f1 Score reported in Table 11, 12, 13, 14 and 15, we find similar conclusion patterns to the accuracy score, while we usually witness a wider gap between *o.o.d.* and *i.i.d.* model performance.

C.10 Agreement and Maintenance Plan

Hosting Platform. We will use Github as the hosting platform of our code. We provide detailed preprocessing Python scripts to guide users to replicate and process data from scratch. We also illustrate methodologies to run full experiment results in the code. We also list the license for each dataset and user guidance in the **Readme** file in that Github.

Dependencies. The benchmark is built upon Python 3.8+ and depends on PyTorch, aif360, fairlearn, xgboost, lightgbm. Besides, it uses numpy, scipy, and pandas for basic data manipulation.

Table 14. Worst target domain Macro-F1 Score of all algorithms on the ACS Income and ACS Pub.Cov datasets. In each setting, we test all algorithms on the 50 American states and report the worst Macro-F1 Score among all 50 target states.

Dataset		ACS INCOME								ACS PUB. COV							
Source State		CA		CT		MA		SD		FL		TX		NE		IN	
		<i>i.d.</i>	<i>o.o.d.</i>	<i>i.d.</i>	<i>o.o.d.</i>	<i>i.d.</i>	<i>o.o.d.</i>	<i>i.d.</i>	<i>o.o.d.</i>	<i>i.d.</i>	<i>o.o.d.</i>	<i>i.d.</i>	<i>o.o.d.</i>	<i>i.d.</i>	<i>o.o.d.</i>	<i>i.d.</i>	<i>o.o.d.</i>
Base Methods	LR	0.804	0.610	0.807	0.597	0.809	0.599	0.714	0.644	0.652	0.478	0.644	0.432	0.653	0.468	0.698	0.514
	SVM	0.795	0.539	0.790	0.505	0.793	0.521	0.698	0.599	0.663	0.493	0.665	0.475	0.698	0.457	0.696	0.559
	MLP	0.814	0.574	0.814	0.591	0.816	0.578	0.734	0.669	0.709	0.527	0.713	0.518	0.698	0.496	0.716	0.569
Tree Ensemble Methods	Random Forest	0.809	0.608	0.812	0.599	0.814	0.595	0.687	0.600	0.715	0.503	0.727	0.484	0.729	0.492	0.746	0.573
	LightGBM	0.811	0.595	0.821	0.584	0.823	0.586	0.732	0.644	0.730	0.545	0.739	0.501	0.745	0.474	0.750	0.601
	XGBoost	0.814	0.602	0.819	0.588	0.822	0.591	0.723	0.632	0.723	0.547	0.730	0.489	0.755	0.525	0.747	0.580
DRO Methods	χ^2 -DRO	0.813	0.583	0.812	0.584	0.816	0.570	0.732	0.669	0.704	0.536	0.697	0.514	0.685	0.544	0.715	0.588
	CVaR-DRO	0.808	0.583	0.812	0.591	0.820	0.584	0.730	0.643	0.693	0.517	0.706	0.509	0.668	0.603	0.700	0.549
	χ^2 -DORO	0.801	0.588	0.804	0.535	0.812	0.543	0.717	0.662	0.526	0.476	0.518	0.431	0.526	0.449	0.516	0.419
	CVaR-DORO	0.802	0.560	0.804	0.543	0.811	0.539	0.720	0.655	0.660	0.481	0.675	0.474	0.559	0.444	0.649	0.562
	Group DRO	0.812	0.605	0.813	0.596	0.817	0.580	0.741	0.677	0.706	0.511	0.717	0.513	0.700	0.504	0.419	0.304
Imbalanced Learning Methods	SUBY	0.807	0.562	0.815	0.574	0.820	0.559	0.719	0.606	0.710	0.642	0.710	0.609	0.704	0.616	0.748	0.660
	RWY	0.812	0.553	0.818	0.576	0.821	0.569	0.733	0.645	0.725	0.646	0.729	0.602	0.736	0.555	0.749	0.654
	SUBG	0.813	0.603	0.816	0.588	0.820	0.584	0.726	0.637	0.719	0.566	0.731	0.552	0.739	0.517	0.742	0.542
	RWG	0.814	0.597	0.819	0.593	0.822	0.588	0.726	0.659	0.723	0.542	0.733	0.485	0.748	0.515	0.746	0.591
	JTT	0.777	0.576	0.781	0.601	0.790	0.602	0.710	0.649	0.711	0.618	0.726	0.574	0.727	0.525	0.718	0.548
	DWR	0.812	0.595	0.816	0.597	0.821	0.579	0.733	0.658	0.721	0.540	0.731	0.492	0.732	0.562	0.741	0.608
Fairness Methods	DP	0.807	0.585	0.810	0.582	0.817	0.593	0.716	0.658	0.727	0.569	0.729	0.507	0.750	0.488	0.742	0.587
	EO	0.813	0.599	0.818	0.590	0.820	0.591	0.721	0.632	0.724	0.544	0.734	0.516	0.737	0.514	0.748	0.601
	EP	0.811	0.596	0.819	0.588	0.821	0.580	0.723	0.646	0.724	0.561	0.731	0.487	0.747	0.539	0.748	0.589
	Exp	0.808	0.586	0.810	0.579	0.818	0.585	0.706	0.626	0.724	0.551	0.729	0.484	0.738	0.476	0.741	0.611
	Threshold	0.766	0.548	0.768	0.570	0.771	0.590	0.665	0.611	0.722	0.548	0.717	0.493	0.714	0.504	0.728	0.568

Table 15. Worst target domain Macro-F1 Score of all algorithms on the ACS Mobility and US Accident datasets. In ACS Mobility, we test all algorithms on the 50 American states and report the worst Macro-F1 Score among all 50 target states. And in US Accident, we choose 13 American states with relatively high sample sizes in testing.

Dataset		ACS Mobility								US Accident							
Source State		NY		CA		MS		PA		CA		FL		TX		MN	
		<i>i.d.</i>	<i>o.o.d.</i>	<i>i.d.</i>	<i>o.o.d.</i>	<i>i.d.</i>	<i>o.o.d.</i>	<i>i.d.</i>	<i>o.o.d.</i>	<i>i.d.</i>	<i>o.o.d.</i>	<i>i.d.</i>	<i>o.o.d.</i>	<i>i.d.</i>	<i>o.o.d.</i>	<i>i.d.</i>	<i>o.o.d.</i>
Base Methods	LR	0.451	0.397	0.462	0.399	0.531	0.450	0.527	0.449	0.800	0.437	0.898	0.489	0.936	0.573	0.855	0.528
	SVM	0.604	0.544	0.592	0.527	0.635	0.489	0.623	0.539	0.793	0.505	0.891	0.568	0.928	0.542	0.880	0.540
	MLP	0.600	0.530	0.622	0.560	0.607	0.551	0.608	0.535	0.827	0.592	0.923	0.595	0.934	0.567	0.886	0.548
Tree Ensemble Methods	Random Forest	0.570	0.482	0.587	0.514	0.641	0.492	0.635	0.510	0.846	0.613	0.932	0.579	0.938	0.584	0.911	0.642
	LightGBM	0.637	0.554	0.625	0.545	0.671	0.531	0.660	0.559	0.851	0.617	0.929	0.582	0.940	0.584	0.918	0.639
	XGBoost	0.637	0.557	0.625	0.566	0.678	0.521	0.664	0.560	0.852	0.620	0.942	0.582	0.939	0.585	0.920	0.636
DRO Methods	χ^2 -DRO	0.613	0.571	0.599	0.539	0.540	0.374	0.606	0.539	0.824	0.596	0.922	0.534	0.933	0.573	0.883	0.534
	CVaR-DRO	0.621	0.551	0.628	0.557	0.574	0.512	0.639	0.518	0.825	0.591	0.924	0.572	0.936	0.582	0.888	0.561
	χ^2 -DORO	0.509	0.464	0.619	0.568	0.530	0.474	0.540	0.481	0.815	0.540	0.920	0.592	0.927	0.569	0.874	0.590
	CVaR-DORO	0.533	0.500	0.625	0.531	0.521	0.479	0.510	0.443	0.825	0.607	0.922	0.569	0.934	0.575	0.887	0.571
	Group DRO	0.588	0.516	0.566	0.480	0.564	0.491	0.595	0.508	N/A	N/A	N/A	N/A	N/A	N/A	N/A	N/A
Imbalanced Learning Methods	SUBY	0.657	0.590	0.649	0.548	0.674	0.565	0.678	0.568	0.854	0.623	0.933	0.585	0.938	0.582	0.915	0.635
	RWY	0.657	0.574	0.647	0.573	0.678	0.557	0.677	0.576	0.856	0.618	0.930	0.581	0.940	0.582	0.920	0.637
	SUBG	0.635	0.546	0.624	0.542	0.672	0.525	0.658	0.552	0.847	0.627	0.925	0.578	0.937	0.582	0.906	0.635
	RWG	0.637	0.542	0.621	0.553	0.676	0.521	0.663	0.539	0.855	0.614	0.929	0.588	0.938	0.583	0.919	0.635
	JTT	0.639	0.555	0.616	0.546	0.660	0.536	0.639	0.528	0.843	0.611	0.922	0.581	0.935	0.583	0.912	0.635
	DWR	0.622	0.553	0.620	0.550	0.656	0.513	0.647	0.561	0.853	0.623	0.929	0.576	0.939	0.583	0.917	0.627
Fairness Methods	DP	0.630	0.555	0.621	0.556	0.663	0.536	0.668	0.557	0.847	0.618	0.922	0.590	0.933	0.582	0.915	0.630
	EO	0.632	0.552	0.625	0.547	0.665	0.549	0.662	0.543	0.846	0.614	0.926	0.584	0.938	0.583	0.917	0.634
	EP	0.633	0.550	0.620	0.552	0.671	0.529	0.660	0.563	0.852	0.621	0.928	0.587	0.937	0.583	0.914	0.636
	Exp	0.633	0.544	0.622	0.551	0.669	0.531	0.663	0.544	0.837	0.613	0.893	0.580	0.909	0.564	0.854	0.619
	Threshold	0.629	0.551	0.620	0.550	0.661	0.528	0.658	0.551	0.820	0.605	0.870	0.583	0.885	0.560	0.809	0.601

Maintenance Plan. The datasets provided here will be maintained by the authors of the paper, which can be contacted by raising an issue on GitHub or by contacting the first authors directly. Our benchmark and a simple open-sourced Python package based on that may be updated at the discretion of authors in the future, which includes more refined algorithm implementations, datasets, and framework with improved efficiency.

Author Statements. To the best of our knowledge, the proposed benchmark is based on existing datasets and does not violate any existing licenses non contain personally identifiable or privacy-related information. And we claim all the responsibility in case of a violation of rights if such a violation were to exist.

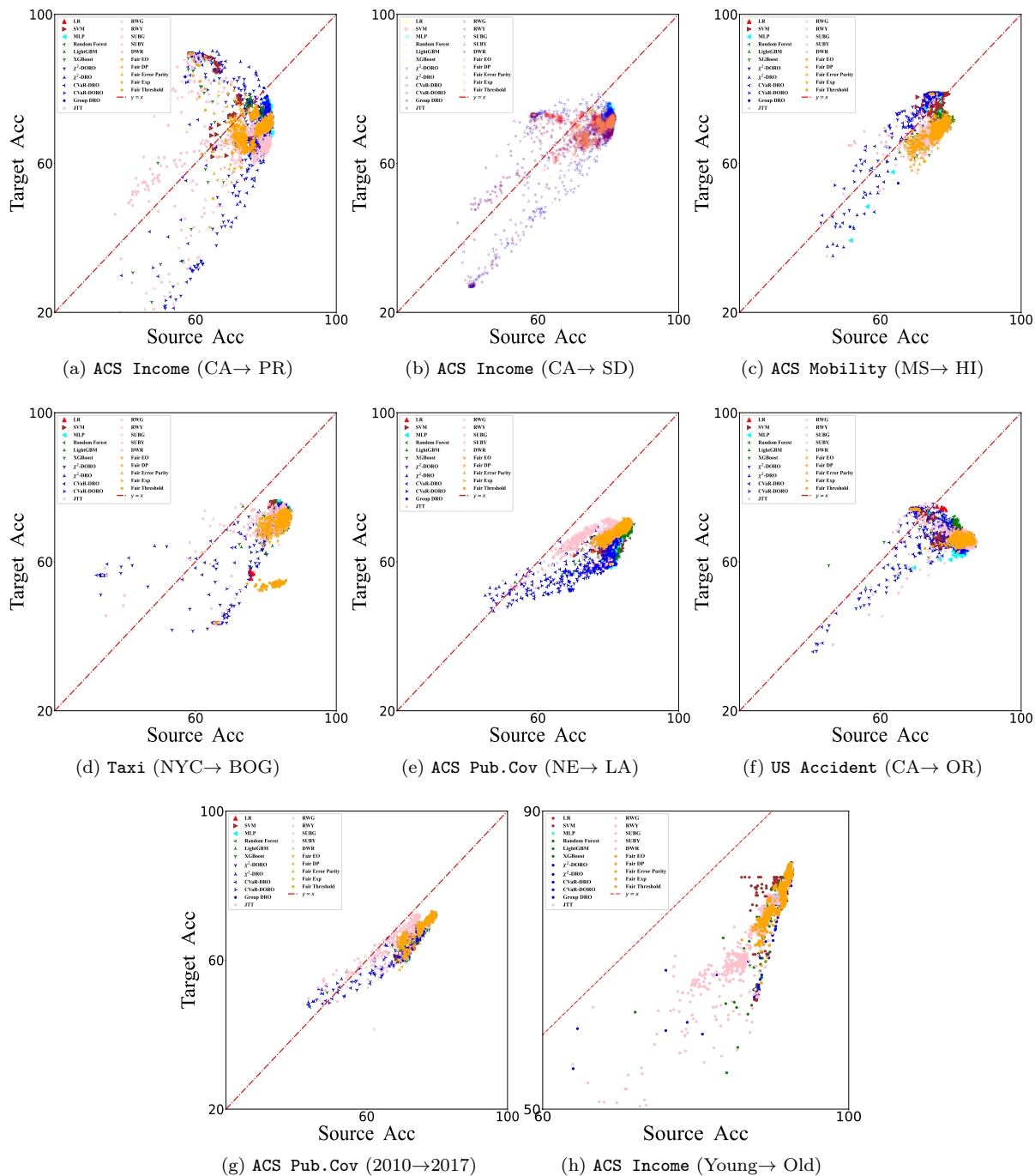


Figure 11. Target vs. source accuracies for 22 algorithms and datasets in our benchmark. Each point represents one hyperparameter configuration. (a)-(b): two examples of ACS Income dataset with California (CA) as the source state, and Puerto Rico (PR) and South Dakota (SD) as targets. (c)-(g): five examples of ACS Mobility, Taxi, ACS Pub.Cov, US Accident datasets. (h): simulated covariate shifts on on sub-sampled ACS Income dataset.